A Multilevel Decoupling Method for the Navier–Stokes/Darcy Model

Prince Chidyagwai[a],

[a]*Department of Mathematics and Statistics, Loyola University Maryland, Baltimore, MD, 21210, U.S.A.*

Abstract

This paper considers a multilevel decoupling method for the coupled Navier–Stokes/Darcy model describing a free flowing fluid over a porous medium. The method utilizes a sequence of meshes on which a low dimensional fully coupled nonlinear problem is solved only on a very coarse initial mesh. On subsequent finer meshes, the approximate solution in each flow region is obtained by solving a linear decoupled problem and performing a correction step. The correction step in each domain is achieved by solving a linear system that differs from the original decoupled system only in the right hand side. We prove optimal error estimates and demonstrate that for a sequence of meshes with spacing $h_j = h_{j-1}^2$, the decoupling method is computationally efficient and achieves the same order of approximation as the fully coupled method.

Keywords: Multilevel method, Navier-Stokes equations, Darcy's law, Coupling interface conditions, Decoupling techniques

1. Introduction

We consider a multilevel decoupling method for the Navier–Stokes/Darcy model. This model has a wide range of applications in science and engineering in scenarios where a free flowing fluid moves over a porous medium. This coupled problem has been studied extensively in the literature; see for example [14, 15, 18, 28–31, 47, 49, 56] and references therein. We mention [28] for an overview of results on the coupled model for approximations based on continuous finite elements (CG), [30, 49] for numerical schemes based on discontinuous Galerkin finite elements (DG) and [18] for a multi-numerics scheme combining CG and DG methods in the free flow and porous media domains, respectively.

The finite element discretization of the fully coupled Navier–Stokes/Darcy model leads to a large, sparse, nonlinear and ill-conditioned algebraic system. Assembling and solving this non-linear system on large domains is computationally expensive; therefore, the development of efficient decoupling techniques is important not only for this problem, but also for other multi-physics couplings that may have the same general form. Indeed, the numerical analysis of coupled problems continues to garner interest in the direction of advancing computational models to be more sophisticated and physically relevant. A few examples include coupled free flow with multiphase flow, coupled dual porosity with free flow modeling flow in shale oil reservoirs, multiscale flow in severe regimes and fluid flow interacting with poroelastic material. We refer the reader to [8, 16, 24, 32, 33, 37, 60] for details on these topics.

The naturally decoupled structure of free flow and porous media flow domains means that the coupled problem lends itself well to numerical techniques that decouple the large nonlinear problem into two smaller subproblems in the respective subdomains. Domain decomposition methods for coupled (Navier–Stokes or Stokes)/Darcy models have been considered for example in [1, 11–13, 25–27, 34]. This paper focusses on the numerical analysis and implementation of a three step multiple mesh decoupling method. This technique requires the solution of a small nonlinear coupled problem only on a very coarse mesh, then on subsequent

Email address: pchidyagwai@loyola.edu (Prince Chidyagwai)

[1]This research is supported in part by the U.S. National Science Foundation under grant DMS-1115269.

finer meshes (up to a desired mesh size), the Navier–Stokes/Darcy model is decoupled into relatively smaller subproblems in each domain. The numerical scheme considered in this work combines the continuous finite element method in the free flow region and the DG method in the porous medium. This choice is motivated by the fact that the regular finite element method is adequate for the free flow regimes considered and DG method is numerically well suited to handle discontinuities that may arise in the porous medium [19]. The DG method also allows for easy implementation of high order approximations and satisfies local mass balance which is an important property for numerical approximation of flow problems in the porous medium.

This multilevel decoupling has been applied to the Stokes/Darcy model in [9] using continuous finite element methods. This method is a natural extension of the two-grid decoupling method considered for example in [38, 46, 52, 57, 59, 61] for the Stokes/Darcy problem and in [10, 20, 22, 29, 39, 53, 60] for the Navier–Stokes/Darcy problem. In the two-grid decoupling method, the fully coupled problem is solved on a coarse grid of size h_0, then on a fine grid of size $h_1 = h_0^2$ or $h_1 = h_0^3$ recently in [39], the problem is decoupled into two smaller subproblems. The decoupling is achieved in one of two ways. A parallel approach in which the solution to the fully coupled problem on the coarse mesh as boundary data on the interface for each decoupled problem on the fine mesh. A sequential approach in which the Darcy problem is decoupled using the coarse mesh free flow velocity and the Darcy pressure on the fine mesh is used as a boundary condition for the decoupled free flow problem.

In this paper we consider a three step multilevel sequential decoupling scheme. The method starts with the solution of a small nonlinear coupled problem on a coarse mesh, then on a sequence of finer meshes, the problem is decoupled into two smaller subproblems. The coarse mesh free flow velocity is used as boundary data on the interface for the porous media flow problem. The resulting solution to the decoupled Darcy problem is then applied as boundary data on the interface for a modified linearized Navier–Stokes problem in the free flow region. In the third stage, the decoupled solutions are corrected on the fine mesh by solving linear systems that differ from the original decoupled problems only in the right hand side. The fine mesh correction step improves the quality of the numerical solution in comparison to the widely studied two-grid method. This correction has been applied to solve the Navier–Stokes problem in [22] and has recently been applied to the two-grid decoupling method for the Navier–Stokes/Darcy problem in [39].

The use of a sequence of intermediate finer meshes in the multilevel method allows for a very coarse initial mesh which means that one needs to solve a smaller nonlinear problem compared to the two-grid method. Further, since the DG method is used to approximate the solution in the porous medium, the resulting linear systems are larger compared to the continuous finite element method therefore the development of efficient decoupling strategies is of interest.

Our numerical experiments demonstrate that this multi-mesh decoupling scheme can result in significant computational savings for large problems. In addition, this technique has the potential to be extended to adaptive mesh refinement techniques between mesh levels. Multilevel finite element methods have been widely used in the literature; see for example [35, 36, 43–45, 58]. In this paper we extend the analysis and implementation of the decoupled multilevel method in [9] to the nonlinear Navier–Stokes/Darcy case with a fine mesh correction. We perform a numerical comparison of the multilevel method to the fully coupled method in terms of accuracy and CPU times.

The paper is organized as follows. The fully coupled model and the corresponding finite element discretization are introduced in Sections 2 and 3, respectively. We introduce the multilevel finite element method and prove the convergence of the method in Sections 4 and 5. In Section 6 we provide numerical examples to demonstrate the convergence, robustness with respect to physical parameters and effectiveness in comparison to the fully coupled method. Conclusions follow.

2. Coupled Navier–Stokes/Darcy Model

Let $\Omega \in \mathbb{R}^2$ be a bounded polygonal domain partitioned into two non-overlapping subdomains Ω_1 and Ω_2; for the free flow and porous media flow regions, respectively. The subdomains Ω_1 and Ω_2 are separated by a polygonal interface Γ_{12}. We denote the boundary of the free flow region by $\Gamma_1 = \partial\Omega \cap \partial\Omega_1$. The boundary of the porous medium ($\Gamma_2 = \partial\Omega \cap \partial\Omega_2$) is partitioned into disjoint sets $\Gamma_{2\mathrm{D}}$ and $\Gamma_{2\mathrm{N}}$, the Dirichlet and Neumann boundary edges, respectively, with the condition $|\Gamma_{2\mathrm{D}}| > 0$. We recall the equations governing the flow in each domain. The flow in Ω_1 is described by the Navier–Stokes equations

$$-\nabla \cdot (2\nu \boldsymbol{D}(\boldsymbol{u}) - p\boldsymbol{I}) + \boldsymbol{u} \cdot \nabla \boldsymbol{u} = \boldsymbol{f}_1, \text{ in } \Omega_1, \tag{2.1a}$$

$$\nabla \cdot \boldsymbol{u} = 0, \text{ in } \Omega_1, \tag{2.1b}$$

$$\boldsymbol{u} = 0, \text{ on } \Gamma_1. \tag{2.1c}$$

The variables $\boldsymbol{u}$ and p denote the Navier–Stokes velocity and pressure, respectively. The coefficient ν is the kinematic viscosity of the fluid, the function $\boldsymbol{f}_1$ is the external force acting on the free fluid and $\boldsymbol{D}(\boldsymbol{u})$ is the rate of strain matrix

$$\boldsymbol{D}(\boldsymbol{u}) = \frac{1}{2}(\nabla \boldsymbol{u} + \boldsymbol{u}^T).$$

The flow in the porous medium is governed by Darcy's Law

$$-\nabla \cdot \boldsymbol{K} \nabla \phi = f_2, \text{ in } \Omega_2, \tag{2.2a}$$

$$\phi = 0, \text{ on } \Gamma_{2\mathrm{D}}, \tag{2.2b}$$

$$\boldsymbol{K} \nabla \phi \cdot \boldsymbol{n}_2 = g_{\mathrm{N}}, \text{ on } \Gamma_{2\mathrm{N}}. \tag{2.2c}$$

The fluid velocity and pressure in Ω_2 are denoted by $\boldsymbol{u}_2$ and ϕ, respectively. We consider a numerical approximation of the Darcy pressure ϕ; with the Darcy velocity $\boldsymbol{u}_2$ obtained by a post processing step by numerically differentiating the pressure as

$$\boldsymbol{u}_2 = -\boldsymbol{K} \nabla \phi.$$

The function f_2 is the external force acting on the fluid and g_{N} is the prescribed flux. The vector $\boldsymbol{n}_2$ denotes the unit vector normal to Γ_2 and the coefficient $\boldsymbol{K}$ is a symmetric positive definite tensor representing the hydraulic conductivity of the porous medium. We define $\boldsymbol{K} = k\boldsymbol{I}$ for a real constant k, modelling isotropic flow in the porous medium. The coupled model is completed by specifying the following interface conditions on Γ_{12}

$$\boldsymbol{u} \cdot \boldsymbol{n}_{12} = -\boldsymbol{K} \nabla \phi \cdot \boldsymbol{n}_{12}, \tag{2.3a}$$

$$\boldsymbol{u} \cdot \boldsymbol{\tau}_{12} = -2\nu G(\boldsymbol{D}(\boldsymbol{u})\boldsymbol{n}_{12}) \cdot \boldsymbol{\tau}_{12}, \tag{2.3b}$$

$$\phi = ((-2\nu \boldsymbol{D}(\boldsymbol{u}) + p\boldsymbol{I})\boldsymbol{n}_{12}) \cdot \boldsymbol{n}_{12}, \tag{2.3c}$$

where $\boldsymbol{n}_{12}$ directed from Ω_1 to Ω_2 and $\boldsymbol{\tau}_{12}$ are the unit normal and tangent vectors on Γ_{12}, respectively. The interface conditions (2.3a)-(2.3c) are the continuity of the normal component of the velocity, the Beavers-Joseph-Saffman law [7, 40, 51] and the balance of forces, respectively. In (2.3b), G is a constant that depends on the nature of the porous medium. The standard weak formulation of (2.1a)-(2.1c), (2.2a)-(2.2c) and (2.3a)-(2.3c) reads

$$\begin{aligned}
&\text{Find } (\boldsymbol{u}, p, \phi) \in (\boldsymbol{X}_1, M_1, M_2) \text{ s.t.} \\
&\forall \boldsymbol{v}_1 \in \boldsymbol{X}_1, \forall q_2 \in M_2, \quad 2\nu\big(\boldsymbol{D}(\boldsymbol{u}), \boldsymbol{D}(\boldsymbol{v}_1)\big)_{\Omega_1} + \big(\boldsymbol{u} \cdot \nabla \boldsymbol{u}, \boldsymbol{v}_1\big)_{\Omega_1} \\
&-\big(p, \nabla \cdot \boldsymbol{v}_1\big)_{\Omega_1} + \frac{1}{G}\big(\boldsymbol{u} \cdot \boldsymbol{\tau}_{12}, \boldsymbol{v}_1 \cdot \boldsymbol{\tau}_{12}\big)_{\Gamma_{12}} - \big(\boldsymbol{u} \cdot \boldsymbol{n}_{12}, q_2\big)_{\Gamma_{12}} \qquad (2.4a) \\
&+(\phi, \boldsymbol{v}_1 \cdot \boldsymbol{n}_{12})_{\Gamma_{12}} + \big(\boldsymbol{K} \nabla \phi, \nabla q_2\big)_{\Omega_2} = \big(\boldsymbol{f}_1, \boldsymbol{v}_1\big)_{\Omega_1} + \big(f_2, q_2\big)_{\Omega_2} + \big(g_{\mathrm{N}}, q_2\big)_{\Gamma_{2\mathrm{N}}}, \\
&\forall q_1 \in M_1, \quad (\nabla \cdot \boldsymbol{u}, q_1)_{\Omega_1} = 0, \qquad (2.4b)
\end{aligned}$$

where $\boldsymbol{X}_1, M_1$ and M_2 are the Navier–Stokes velocity, pressure and Darcy pressure function spaces, respectively. We list the spaces

$$\begin{aligned}
\boldsymbol{X}_1 &= \{\boldsymbol{v}_1 \in (H^1(\Omega_1))^2 : \boldsymbol{v}_1 = 0 \text{ on } \Gamma_1\}, \\
M_1 &= L^2(\Omega_1), \\
M_2 &= \{q_2 \in H^1(\Omega_2) : q_2 = 0 \text{ on } \Gamma_{2\mathrm{D}}\}.
\end{aligned}$$

We refer the reader to [18] for details of the derivation and analysis of the weak formulation (2.4a)-(2.4b).

3. Finite element discretization

Let $\mathcal{E}^h = \mathcal{E}_1^h \cup \mathcal{E}_2^h$ be a regular [21] triangulation of the subdomains $\overline{\Omega}_1 \cup \overline{\Omega}_2$ dependent on a mesh parameter h. The Navier–Stokes velocity and pressure in Ω_1 are approximated by conforming finite element spaces $\boldsymbol{X}_1^h \subset \boldsymbol{X}_1$ and $M_1^h \subset M_1$, respectively, satisfying the discrete inf-sup stability condition

$$\inf_{q_1 \in M_1^h} \sup_{\boldsymbol{v}_1 \in \boldsymbol{X}_1^h} \frac{(q_1, \nabla \cdot \boldsymbol{v}_1)_{\Omega_1}}{||\nabla \boldsymbol{v}_1||_{L^2(\Omega_1)} ||q_1||_{L^2(\Omega_1)}} \geq \beta_\star > 0 \tag{3.1}$$

where $\beta_\star$ is a constant. The free flow velocity and pressure are approximated using the first order MINI element [5]. The Darcy pressure is approximated by the space of discontinuous polynomials of degree k_2

$$M_2^h = \{q_2 \in L^2(\Omega_2) : \forall E \in \mathcal{E}_2^h, q_2|_E \in \mathbb{P}_{k_2}(E)\}.$$

Following the standard DG notation in $\mathcal{E}_2^h$, we denote the interior edges of $\mathcal{E}_2^h$ by Γ_2^h and associate each edge with a unit normal vector $\boldsymbol{n}_e$. In the case of boundary edges $\boldsymbol{n}_e$ is taken to be the outward normal vector. For interior edges with neighbors E_i^e and E_j^e, there are two traces of q_2 along e. For a given $\boldsymbol{n}_e$ pointing from E_i^e to E_j^e we denote the average $\{q_2\}$ and jump $[q_2]$ of a piecewise discontinuous polynomial q_2 by

$$\{q_2\} = \frac{1}{2}(q_2|_{E_i^e}) + \frac{1}{2}(q_2|_{E_j^e}), \qquad [q_2] = (q_2|_{E_i^e}) - (q_2|_{E_j^e}), \quad \forall e = \partial E_i^e \cap \partial E_j^e.$$

The space M_2^h is equipped with the standard DG norm

$$\forall q_2 \in M_2^h, \quad ||q_2||_{\mathrm{DG}} = \left(\sum_{E \in \mathcal{E}_2^h} ||\boldsymbol{K}^{1/2} \nabla q_2||^2_{L^2(E)} + \sum_{e \in \Gamma_h^2} \frac{1}{|e|} ||[q_2]||^2_{L^2(e)} \right)^{1/2}.$$

We refer the reader to [48] for details of the DG method. The multinumerics scheme combining the continuous and discontinuous finite element methods has been shown to be well suited to capture both the flow in the Navier–Stokes region and in porous media that may contain discontinuities in the hydraulic conductivity [19]. The use of a multi-numerics scheme also serves to illustrate the flexibility of the decoupling scheme. Specifically, optimized numerical schemes for each decoupled problem may be used in each subdomain.

For compactness, we introduce the following bilinear and trilinear forms representing discretizations of terms in the coupled weak formulation (2.4a)-(2.4b). The discretization of the Navier–Stokes viscous term and pressure terms are denoted by a_{NS} and b_{NS}, respectively:

$$\begin{aligned} \forall \boldsymbol{v}, \boldsymbol{w} \in \boldsymbol{X}_1^h, \quad & a_{\mathrm{NS}}(\boldsymbol{v}, \boldsymbol{w}) = 2\nu(\boldsymbol{D}(\boldsymbol{v}), \boldsymbol{D}(\boldsymbol{w}))_{\Omega_1}, \\ \forall \boldsymbol{v} \in \boldsymbol{X}_1^h, \forall q_1 \in M_1^h, \quad & b_{\mathrm{NS}}(\boldsymbol{v}, q_1) = -(q_1, \nabla \cdot \boldsymbol{v})_{\Omega_1}. \end{aligned} \tag{3.2}$$

The discretization of the nonlinear term is denoted by c_{NS}

$$\begin{gathered} \forall \boldsymbol{z}, \boldsymbol{v}, \boldsymbol{w} \in \boldsymbol{X}_1^h, \\ c_{\mathrm{NS}}(\boldsymbol{z}, \boldsymbol{v}, \boldsymbol{w}) = \frac{1}{2}(\boldsymbol{z} \cdot \nabla \boldsymbol{v}, \boldsymbol{w})_{\Omega_1} - \frac{1}{2}(\boldsymbol{z} \cdot \nabla \boldsymbol{w}, \boldsymbol{v})_{\Omega_1} + \frac{1}{2}(\boldsymbol{z} \cdot \boldsymbol{n}_{12}, \boldsymbol{v} \cdot \boldsymbol{w})_{\Gamma_{12}}. \end{gathered} \tag{3.3}$$

The discretization of the diffusion term in the Darcy equations is denoted by the bilinear form a_{D}

$$\begin{aligned} \forall q_2, t_2 \in M_2^h, \quad a_{\mathrm{D}}(q_2, t_2) = & \sum_{E \in \mathcal{E}_2^h} \big(\boldsymbol{K} \nabla q_2, \nabla t_2\big)_E - \sum_{e \in \Gamma_2^h} \big(\{\boldsymbol{K} \nabla q_2 \cdot \boldsymbol{n}_e\}, [t_2]\big)_e \\ & + \epsilon \sum_{e \in \Gamma_h^2} \big(\{\boldsymbol{K} \nabla t_2 \cdot \boldsymbol{n}_e\}, [q_2]\big)_e + \sum_{e \in \Gamma_h^2} \frac{\sigma_e}{|e|} \big([q_2], [t_2]\big)_e. \end{aligned} \tag{3.4}$$

In the definition of a_{D} we use the interior penalty discontinuous Galerkin method [4, 6, 23, 50, 55]. The parameter $\epsilon \in \{-1, 0, 1\}$ and $\sigma_e \geq 0$ is a penalty parameter that varies with respect to the edge in $\mathcal{E}_2^h$. The bilinear form a_{D} is coercive and corresponds to the nonsymmetric interior penalty Galerkin method (NIPG) ($\epsilon = 1$), symmetric interior penalty Galerkin method (SIPG) ($\epsilon = -1$) or the incomplete interior penalty Galerkin method (IIPG) ($\epsilon = 0$) methods. The terms involving interface coupling are defined by γ_{12}

$$\forall \boldsymbol{v}, \boldsymbol{w} \in \boldsymbol{X}_1^h \quad \forall q_2, t_2 \in M_2^h,$$
$$\gamma_{12}(\boldsymbol{v}, q_2; \boldsymbol{w}, t_2) = \big(q_2, \boldsymbol{w} \cdot \boldsymbol{n}_{12}\big)_{\Gamma_{12}} + \frac{1}{G}\big(\boldsymbol{v} \cdot \boldsymbol{\tau}_{12}, \boldsymbol{w} \cdot \boldsymbol{\tau}_{12}\big)_{\Gamma_{12}} - \big(\boldsymbol{v} \cdot \boldsymbol{n}_{12}, t_2\big)_{\Gamma_{12}}.$$

We define the linear form L to incorporate the source and data terms

$$\forall \boldsymbol{v} \in \boldsymbol{X}_1^h, \quad \forall q_2 \in M_2^h,$$
$$L(\boldsymbol{v}, q_2) = \big(\boldsymbol{f}_1, \boldsymbol{v}\big)_{\Omega_1} + (f_2, q_2)_{\Omega_2} + \sum_{e \in \Gamma_{2\mathrm{N}}} (g_{\mathrm{N}}, q_2)_e.$$

On a mesh of size h, the finite element discretization of the fully coupled Navier–Stokes/Darcy problem reads

$$\text{Find } (\boldsymbol{U}^h, P^h, \phi^h) \in (\boldsymbol{X}_1^h, M_1^h, M_2^h) \text{ s.t. } \forall \boldsymbol{v}_1 \in \boldsymbol{X}_1^h, \forall q_2 \in M_2^h,$$
$$a_{\mathrm{NS}}(\boldsymbol{U}^h, \boldsymbol{v}_1) + b_{\mathrm{NS}}(\boldsymbol{v}_1, P^h) + c_{\mathrm{NS}}(\boldsymbol{U}^h; \boldsymbol{U}^h, \boldsymbol{v}_1) \tag{3.5a}$$
$$+ a_{\mathrm{D}}(\phi^h, q_2) + \gamma_{12}(\boldsymbol{U}^h, \phi^h; \boldsymbol{v}_1, q_2) = L(\boldsymbol{v}_1, q_2),$$
$$\forall q_1 \in M_1^h, \quad b_{\mathrm{NS}}(\boldsymbol{U}^h, q_1) = 0. \tag{3.5b}$$

The convergence of successive iterative schemes for the coupled Navier–Stokes/Darcy problem has been shown in [30]. We solve the nonlinear system, (3.5a)-(3.5b) using the following Newton linearization scheme starting with an initial guess $\boldsymbol{U}_0^h = \boldsymbol{0}$ and a stopping criterion $||\boldsymbol{U}_n^h - \boldsymbol{U}_{n-1}^h||_{L^2(\Omega_1)} < 10^{-9}$ as follows

$$\text{Find } (\boldsymbol{U}_n^h, P_n^h, \phi_n^h) \in (\boldsymbol{X}_1^h, M_1^h, M_2^h) \text{ s.t. } \forall \boldsymbol{v}_1 \in \boldsymbol{X}_1^h, \forall q_2 \in M_2^h,$$
$$a_{\mathrm{NS}}(\boldsymbol{U}_n^h, \boldsymbol{v}_1) + b_{\mathrm{NS}}(\boldsymbol{v}_1, P_n^h) + c_{\mathrm{NS}}(\boldsymbol{U}_{n-1}^h; \boldsymbol{U}_n^h, \boldsymbol{v}_1)$$
$$+ c_{\mathrm{NS}}(\boldsymbol{U}_n^h; \boldsymbol{U}_{n-1}^h, \boldsymbol{v}_1) + a_{\mathrm{D}}(\phi_n^h, q_2) \tag{3.6a}$$
$$+ \gamma_{12}(\boldsymbol{U}_n^h, \phi_n^h; \boldsymbol{v}_1, q_2) = L(\boldsymbol{v}_1, q_2) + c_{\mathrm{NS}}(\boldsymbol{U}_{n-1}^h; \boldsymbol{U}_{n-1}^h, \boldsymbol{v}_1),$$
$$\forall q_1 \in M_1^h, \quad b_{\mathrm{NS}}(\boldsymbol{U}_n^h, q_1) = 0. \tag{3.6b}$$

Since the solution of the fully coupled problem is computed on a single mesh, we will refer to it as the one-level method. We note that each iteration in (3.6a)-(3.6b) requires the solution of a large, coupled, ill-conditioned algebraic system that presents a numerical challenges to solve. This makes the decoupling schemes attractive as they result in relatively smaller systems on each domain.

4. Multilevel finite element method

In this section we describe the three step multilevel finite element method for the coupled Navier–Stokes/Darcy system. We consider a sequence of $J+1$ meshes with spacing $h_j, j = 0, 1, \ldots, J$ such that $h_0 > h_1 > \cdots > h_J$. For each mesh of size h_j, let $\boldsymbol{X}^{h_j}, M_1^{h_j}$ and $M_2^{h_j}$ be the finite element spaces corresponding to the Navier–Stokes velocity, pressure and Darcy pressure, respectively for each mesh size h_j with

$$(\boldsymbol{X}_1^{h_0} \times M_1^{h_0} \times M_2^{h_0}) \subset (\boldsymbol{X}_1^{h_1} \times M_1^{h_1} \times M_2^{h_1}) \subset \cdots \subset (\boldsymbol{X}_1^{h_J} \times M_1^{h_J} \times M_2^{h_J}).$$

The $(J+1)$-level method begins by solving the fully coupled nonlinear problem, (3.5a)-(3.5b) on a coarse mesh with size h_0, then on a sequence of finer grids of mesh size h_j (for $1 \le j \le J$), two smaller problems are solved in each subdomain. First, a Darcy problem to obtain the approximate Darcy pressure $\phi_{h_j}^* \in M_2^{h_j}$, using the Navier–Stokes velocity $\boldsymbol{U}_{h_{j-1}} \in X^{h_{j-1}}$ as a boundary condition on the interface. Second, a Navier–Stokes problem linearized about $\boldsymbol{U}_{h_{j-1}}$ with the Darcy decoupled solution $\phi^*_{h_j}$ applied as boundary data on the interface to obtain $(\boldsymbol{U}^*_{h_j}, P^*_{h_j})$. The approximate solutions are interpolated between mesh levels. The third step of the method corrects the Darcy pressure solution $\phi^*_{h_j}$ by using the Navier–Stokes velocity $\boldsymbol{U}^*_{h_j}$ and finally the Navier–Stokes velocity and pressure are corrected using ϕ_{h_j} on the interface to obtain $(\boldsymbol{U}_{h_j}, P_{h_j})$. We note that the correction problems differ from the decoupled problems in the right hand side and thus are not computationally expensive. The multilevel decoupled method is summarized below.

Fully coupled step on mesh h_0

Step 1. Solve a small fully coupled nonlinear problem on coarsest mesh h_0

$$\begin{aligned}
&\text{Find } (\boldsymbol{U}^{h_0}, P^{h_0}, \phi^{h_0}) \in (\boldsymbol{X}_1^{h_0} \times M_1^{h_0} \times M_2^{h_0}) \text{ s.t. } \forall \boldsymbol{v} \in \boldsymbol{X}_1^{h_0}, \forall q_2 \in M_2^{h_0},\\
&a_{\mathrm{NS}}(\boldsymbol{U}^{h_0}, \boldsymbol{v}_1) + b_{\mathrm{NS}}(\boldsymbol{v}_1, P^{h_0}) + c_{\mathrm{NS}}(\boldsymbol{U}^{h_0}; \boldsymbol{U}^{h_0}, \boldsymbol{v}_1)\\
&+\gamma_{12}(\boldsymbol{U}^{h_0}, \phi_2^{h_0}; \boldsymbol{v}_1, q_2) + a_{\mathrm{D}}(\phi^{h_0}, q_2) = L(\boldsymbol{v}_1, q_2) \qquad (4.1\text{a})\\
&\forall q_1 \in M_1^{h_0}, \quad b_{\mathrm{NS}}(\boldsymbol{U}^{h_0}, q_1) = 0. \qquad (4.1\text{b})
\end{aligned}$$

Decoupling steps on a sequence of meshes $h_j, 1 \leq j \leq J$

Step 2. Solve two decoupled problems on mesh h_j

(i) Darcy problem with $\boldsymbol{U}_{h_{j-1}}$ as boundary data on Γ_{12} :

$$\begin{aligned}
&\text{Find } \phi^*_{h_j} \in M_2^{h_j} \text{ s.t. } \forall q_2 \in M_2^{h_j},\\
&a_{\mathrm{D}}(\phi^*_{h_j}, q_2) = (f_2, q_2)_{\Omega_2} + (\boldsymbol{U}_{h_{j-1}} \cdot \boldsymbol{n}_{12}, q_2)_{\Gamma_{12}} + \sum_{e \in \Gamma_{2\mathrm{N}}} (g_{\mathrm{N}}, q_2)_e. \qquad (4.2)
\end{aligned}$$

(ii) Navier–Stokes problem linearized about $\boldsymbol{U}_{h_{j-1}}$ with $\phi^*_{h_j}$ as boundary data on Γ_{12} :

$$\begin{aligned}
&\text{Find } (\boldsymbol{U}^*_{h_j}, P^*_{h_j}) \in (\boldsymbol{X}_1^{h_j}, M_1^{h_j}) \text{ s.t. } \forall \boldsymbol{v}_1 \in \boldsymbol{X}_1^{h_j}, \forall q_1 \in M_1^{h_j},\\
&a_{\mathrm{NS}}(\boldsymbol{U}^*_{h_j}, \boldsymbol{v}_1) + b_{\mathrm{NS}}(\boldsymbol{v}_1, P^*_{h_j}) + c_{\mathrm{NS}}(\boldsymbol{U}_{h_{j-1}}; \boldsymbol{U}^*_{h_j}, \boldsymbol{v}_1)\\
&+c_{\mathrm{NS}}(\boldsymbol{U}^*_{h_j}; \boldsymbol{U}_{h_{j-1}}, \boldsymbol{v}_1) + \frac{1}{G}\left(\boldsymbol{U}^*_{h_j} \cdot \boldsymbol{\tau}_{12}, \boldsymbol{v}_1 \cdot \boldsymbol{\tau}_{12}\right)_{\Gamma_{12}} \qquad (4.3\text{a})\\
&= (\boldsymbol{f}_1, \boldsymbol{v}_1)_{\Omega_1} + c_{\mathrm{NS}}(\boldsymbol{U}_{h_{j-1}}; \boldsymbol{U}_{h_{j-1}}, \boldsymbol{v}_1) - (\phi^*_{h_j}, \boldsymbol{v}_1 \cdot \boldsymbol{n}_{12})_{\Gamma_{12}}\\
&\forall q_1 \in M_1^{h}, \quad b_{\mathrm{NS}}(\boldsymbol{U}^*_{h_j}, q_1) = 0. \qquad (4.3\text{b})
\end{aligned}$$

Step 3. Solve two *correction* subproblems on mesh h_j

(i) Darcy problem with $\boldsymbol{U}^*_{h_j}$ as boundary data on Γ_{12} :

$$\begin{aligned}
&\text{Find } \phi_{h_j} \in M_2^{h_j} \text{ s.t. } \forall q_2 \in M_2^{h_j},\\
&a_{\mathrm{D}}(\phi_{h_j}, q_2) = (f_2, q_2)_{\Omega_2} + (\boldsymbol{U}^*_{h_j} \cdot \boldsymbol{n}_{12}, q_2)_{\Gamma_{12}} + \sum_{e \in \Gamma_{2\mathrm{N}}} (g_{\mathrm{N}}, q_2)_e. \qquad (4.4)
\end{aligned}$$

(ii) Correct Navier–Stokes velocity and pressure with ϕ_{h_j} as boundary data on Γ_{12} :

$$
\begin{aligned}
&\text{Find } (\boldsymbol{U}_{h_j}, P_{h_j}) \in (\boldsymbol{X}_1^{h_j}, M_1^{h_j}) \text{ s.t. } \forall \boldsymbol{v}_1 \in \boldsymbol{X}_1^{h_j}, \forall q_1 \in M_1^{h_j},\\
&a_{\mathrm{NS}}(\boldsymbol{U}_{h_j}, \boldsymbol{v}_1) + b_{\mathrm{NS}}(\boldsymbol{v}_1, P_{h_j}) + c_{\mathrm{NS}}(\boldsymbol{U}_{h_{j-1}}; \boldsymbol{U}_{h_j}, \boldsymbol{v}_1)\\
&+c_{\mathrm{NS}}(\boldsymbol{U}_{h_j}; \boldsymbol{U}_{h_{j-1}}, \boldsymbol{v}_1) + \frac{1}{G}(\boldsymbol{U}_{h_j} \cdot \boldsymbol{\tau}_{12}, \boldsymbol{v}_1 \cdot \boldsymbol{\tau}_{12})_{\Gamma_{12}} \qquad (4.5a)\\
&= (\boldsymbol{f}_1, \boldsymbol{v}_1)_{\Omega_1} + c_{\mathrm{NS}}(\boldsymbol{U}_{h_{j-1}}; \boldsymbol{U}^*_{h_j}, \boldsymbol{v}_1) + c_{\mathrm{NS}}(\boldsymbol{U}^*_{h_j}, \boldsymbol{U}_{h_{j-1}} - \boldsymbol{U}^*_{h_j}, \boldsymbol{v}_1) - (\phi_{h_j}, \boldsymbol{v}_1 \cdot \boldsymbol{n}_{12})_{\Gamma_{12}}\\
&\forall q_1 \in M_1^h, \quad b_{\mathrm{NS}}(\boldsymbol{U}_{h_j}, q_1) = 0. \qquad (4.5b)
\end{aligned}
$$

Remark 1. We note that Step 2 can also be implemented in parallel by using the Darcy pressure from the coarse mesh $\phi_{h_{j-1}}$ on the interface in (4.3a). This form of the decoupling scheme has been widely used in the literature. Optimal convergence results for the parallel two-grid Stokes/Darcy decoupling can be found in [38]. In this work, we choose the decoupling technique analyzed in [41, 53, 57, 61] and use $\phi^*_{h_j}$ as a boundary condition for the fluid region due to a sequential code. In addition, our numerical tests indicate that this approach yields a more accurate solution.

5. Stability and Convergence analysis

In this section we prove the stability and convergence for the multilevel method and establish the appropriate mesh spacing that ensures that the decoupling method converges with the same order as the fully coupled approach. In the following analysis we assume that the velocity and pressure are approximated by inf-sup stable first order MINI element and the Darcy pressure is approximated by linear discontinuous elements. We begin by recalling the Poincaré and Korn's inequalities and trace and Sobolev inequalities – there exist constants $\mathcal{P}_1, C_0, C_1, C_2$ depending on Ω_1 and $\mathcal{P}_2$, C_3, C_4 depending on Ω_2 such that for all $\boldsymbol{v} \in \boldsymbol{X}_1^h$,

$$||\boldsymbol{v}||_{L^2(\Omega_1)} \leq \mathcal{P}_1 |\boldsymbol{v}|_{H^1(\Omega_1)}, \quad ||\boldsymbol{v}||_{L^2(\Gamma_{12})} \leq C_0 |\boldsymbol{v}|_{H^1(\Omega_1)}, \quad |\boldsymbol{v}|_{H^1(\Omega_1} \leq C_1 ||\boldsymbol{D}(\boldsymbol{v})||_{L^2(\Omega_1)}, \tag{5.1}$$

and for $q_2 \in M_2^h$,

$$||q_2||_{L^2(\Omega_2)} \leq \mathcal{P}_2 ||q_2||_{\mathrm{DG}}, \quad ||q_2||_{L^2(\Gamma_{12})} \leq C_2 ||q_2||_{\mathrm{DG}}, \quad ||q_2||_{L^2(\Gamma_{2\mathrm{N}})} \leq C_3 ||q_2||_{\mathrm{DG}}. \tag{5.2}$$

We also state the following results on the continuity of the bilinear form c_{NS}, stability and convergence of the numerical solution to the fully coupled Navier–Stokes/Darcy problem, (3.5a)-(3.5b) and coercivity of a_{D} and refer the reader to [4, 6, 17, 18, 23, 30, 50, 54, 55] for proofs.

Lemma 1. *Assuming the domain Ω_1 is of class C^1 and regular enough, the trilinear form c_{NS} defined in* (3.3) *is continuous. There exists a constant C_4 depending on Ω_1 such that*

$$c_{\mathrm{NS}}(\boldsymbol{z}_1; \boldsymbol{v}_1, \boldsymbol{w}_1) \leq C_4 \begin{cases} ||\boldsymbol{D}(\boldsymbol{z}_1)||_{L^2(\Omega_1)} ||\boldsymbol{D}(\boldsymbol{v}_1)||_{L^2(\Omega_1)} ||\boldsymbol{D}(\boldsymbol{w}_1)||_{L^2(\Omega_1)} & \forall \boldsymbol{z}_1, \boldsymbol{v}_1, \boldsymbol{w}_1 \in \boldsymbol{X}_1^h \\ ||\boldsymbol{z}_1||_{L^2(\Omega_1)} ||\boldsymbol{D}(\boldsymbol{v}_1)||_{L^2(\Omega_1)} ||\boldsymbol{w}_1||_{H^2(\Omega_1)} & \forall \boldsymbol{z}_1, \boldsymbol{v}_1 \in \boldsymbol{X}_1^h, \boldsymbol{w}_1 \in H^2(\Omega_1) \\ ||\boldsymbol{D}(\boldsymbol{z}_1)||_{L^2(\Omega_1)} ||\boldsymbol{v}_1||_{L^2(\Omega_1)} ||\boldsymbol{w}_1||_{H^2(\Omega_1)} & \forall \boldsymbol{z}_1, \boldsymbol{v}_1 \in \boldsymbol{X}_1^h, \boldsymbol{w}_1 \in H^2(\Omega_1) \end{cases} \tag{5.3}$$

Lemma 2. *The bilinear form a_{D} defined in* (3.4) *is coercive. There exists a constant $\kappa > 0$ independent of h_j such that*

$$\forall q_2 \in M_2^h, \kappa ||q_2||^2_{\mathrm{DG}} \leq a_{\mathrm{D}}(q_2, q_2)$$

Lemma 3. *Let $(\boldsymbol{U}^h, P^h, \phi^h) \in (\boldsymbol{X}_1^h, M_1^h, M_2^h)$ be the solution from the fully coupled scheme* (3.5a)-(3.5b). *Then under the assumption of a small data condition there exists a constant C independent of h such that*

$$||\boldsymbol{D}(\boldsymbol{u} - \boldsymbol{U}^h)||_{L^2(\Omega_1)} + ||p - P^h||_{L^2(\Omega_1)} + ||\phi - \phi^h||_{\mathrm{DG}} \leq Ch$$
$$||(\boldsymbol{u} - \boldsymbol{U}^h)||_{L^2(\Omega_1)} + ||\phi - \phi^h||_{L^2(\Omega_2)} \leq Ch^2$$

In addition, the following stability bound holds:

$$2\nu||D(\boldsymbol{U}^h)||^2_{L^2(\Omega_1)} + \kappa||\phi^h||^2_{\mathrm{DG}} \leq \mathcal{R}^2$$

where $\mathcal{R}$ depends on the Navier–Stokes and Darcy data functions, Poincaré, Korn, Sobolev and trace inequalities.

We begin with the stability and convergence of the two-level method and extend to the multilevel method by induction. The stability of the two-grid Stokes–Darcy solution has been shown in [61], here we extend to the nonlinear Navier-Stokes/Darcy case. For simplicity we consider the homogeneous boundary condition on $\Gamma_{2\mathrm{D}}$ in Ω_2, the non-homogeneous case can be handled by the usual lift argument. We will use C to denote arbitrary constants independent of h.

Lemma 4. *Let $(\boldsymbol{U}^*_{h_1}, P^*_{h_1}, \phi^*_{h_1})$, $(\boldsymbol{U}_{h_1}, P_{h_1}, \phi_{h_1}) \in (\boldsymbol{X}_1^{h_1}, M_1^{h_1}, M_2^{h_1})$ be the solutions to* (4.2)-(4.3b) *and* (4.4)-(4.5b), *respectively i.e. the two-level method with coarse mesh h_0 and fine mesh h_1, then under the condition*

$$\nu^{\frac{3}{2}} > \sqrt{2} C_4 \mathcal{R} \tag{5.4}$$

the velocity and pressure solutions satisfy

$$\kappa||\phi^*_{h_1}||^2_{\mathrm{DG}} \leq (\mathcal{D}^*_1)^2 \tag{5.5a}$$
$$2\nu||\boldsymbol{D}(\boldsymbol{U}^*_{h_1})||^2_{L^2(\Omega_1)} \leq (\mathcal{N}^*_1)^2 \tag{5.5b}$$
$$\kappa||\phi_{h_1}||^2_{\mathrm{DG}} \leq \mathcal{D}_1^2, \tag{5.5c}$$
$$2\nu||\boldsymbol{D}(\boldsymbol{U}_{h_1})||^2_{L^2(\Omega_1)} \leq \mathcal{N}_1^2, \tag{5.5d}$$

where $\mathcal{R}$ is the constant in Lemma 3 and

$$\begin{aligned}
\mathcal{D}^*_1 &= \left[\frac{3}{\kappa}\left(\mathcal{P}_2^2||f_2||^2_{L^2(\Omega_2)} + (C_0C_1C_2)^2\frac{\mathcal{R}^2}{2\nu} + C_3^2||g_{\mathrm{N}}||^2_{L^2(\Gamma_{2\mathrm{N}})}\right)\right]^{\frac{1}{2}} \\
\mathcal{N}^*_1 &= \left[\frac{3}{\nu}\left((\mathcal{P}_1C_1)^2||\boldsymbol{f}_1||^2_{L^2(\Omega_1)} + C_4^2\frac{\mathcal{R}^4}{4\nu^2} + (C_0C_1C_2)^2\frac{(\mathcal{D}^*_1)^2}{\kappa}\right)\right]^{\frac{1}{2}}. \\
\mathcal{D}_1 &= \left[\frac{3}{\kappa}\left(\mathcal{P}_2^2||f_2||^2_{L^2(\Omega_2)} + (C_0C_1C_2)^2\frac{(\mathcal{N}^*_1)^2}{2\nu} + C_3^2||g_{\mathrm{N}}||^2_{L^2(\Gamma_{2\mathrm{N}})}\right)\right]^{\frac{1}{2}} \\
\mathcal{N}_1 &= \left[\frac{3}{\nu}\left((\mathcal{P}_1C_1)^2||\boldsymbol{f}_1||^2_{L^2(\Omega_1)} + \left\{C_4\frac{\mathcal{N}^*_1}{\sqrt{2\nu}}\left(\frac{\mathcal{R}}{\sqrt{2\nu}} + ||\boldsymbol{D}(\boldsymbol{U}_{h_0} - \boldsymbol{U}^*_{h_1})||_{L^2(\Omega_1)}\right)\right\}^2 + (C_0C_1C_2)^2\frac{\mathcal{D}_1^2}{\kappa}\right)\right]^{\frac{1}{2}}.
\end{aligned}$$

Further, if $h_1 = h_0^2$ then we have the following error bounds

$$||\phi - \phi^*_{h_1}||_{\mathrm{DG}} \leq C(h_0^2 + h_1) \leq Ch_1, \tag{5.6a}$$
$$||\boldsymbol{D}(\boldsymbol{u} - \boldsymbol{U}^*_{h_1})||_{L^2(\Omega_1)} + ||p - P^*_{h_1}||_{L^2(\Omega_1)} \leq C(h_0^2 + h_1) \leq Ch_1, \tag{5.6b}$$
$$||\boldsymbol{u} - \boldsymbol{U}^*_{h_1}||_{L^2(\Omega_1)} \leq C(h_0^3 + h_1^2) \leq Ch_1^{\frac{3}{2}}. \tag{5.6c}$$

$$||\phi - \phi_{h_1}||_{\mathrm{DG}} \leq C(h_0^3 + h_1) \leq Ch_1, \tag{5.7a}$$
$$||\boldsymbol{D}(\boldsymbol{u} - \boldsymbol{U}_{h_1})||_{L^2(\Omega_1)} + ||p - P_{h_1}||_{L^2(\Omega_1)} \leq C(h_0^3 + h_1) \leq Ch_1. \tag{5.7b}$$
$$||\boldsymbol{u} - \boldsymbol{U}_{h_1}||_{L^2(\Omega_1)} \leq C(h_0^4 + h_1^2) \leq Ch_1^2. \tag{5.7c}$$

PROOF. Starting with Step 2 of the two-grid decoupling method. We choose $q_2 = \phi^*_{h_1}$ in (4.2) so that

$$a_{\mathrm{D}}(\phi^*_{h_1}, \phi^*_{h_1}) = (f_2, \phi^*_{h_1})_{\Omega_2} + (\boldsymbol{U}_{h_0} \cdot \boldsymbol{n}_{12}, \phi^*_{h_1})_{\Gamma_{12}} + \sum_{e\in\Gamma_{2\mathrm{N}}} (g_{\mathrm{N}}, \phi^*_{h_1})_e. \tag{5.8}$$

We bound the terms in (5.8); using Cauchy–Schwarz and Young's inequalities and inequalities in (5.1)-(5.2). Indeed,

$$\big|(f_2, \phi^*_{h_1})_{\Omega_2}\big| \le \frac{3}{2\kappa}\mathcal{P}_2^2||f_2||^2_{L^2(\Omega_2)} + \frac{\kappa}{6}||\phi^*_{h_1}||^2_{\mathrm{DG}}, \tag{5.9a}$$

$$\big|(\boldsymbol{U}_{h_0} \cdot \boldsymbol{n}_{12}, \phi^*_{h_1})_{\Gamma_{12}}\big| \le \frac{3}{2\kappa}(C_0C_1C_2)^2||\boldsymbol{D}(\boldsymbol{U}_{h_0})||^2_{L^2(\Omega_1)} + \frac{\kappa}{6}||\phi^*_{h_1}||^2_{\mathrm{DG}}, \tag{5.9b}$$

$$\big|(g_{\mathrm{N}}, \phi^*_{h_1})_{\Gamma_{12}}\big| \le \frac{3}{2\kappa}C_3^2||g_{\mathrm{N}}||^2_{L^2(\Gamma_{2\mathrm{N}})} + \frac{\kappa}{6}||\phi^*_{h_1}||^2_{\mathrm{DG}}. \tag{5.9c}$$

Combining Lemma 2 and the bounds (5.9a)-(5.9c) in (5.8) it follows that

$$\frac{\kappa}{2}||\phi^*_{h_1}||^2_{\mathrm{DG}} \le \frac{3}{2\kappa}\Big(\mathcal{P}_2^2||f_2||^2_{L^2(\Omega_2)} + (C_0C_1C_2)^2||\boldsymbol{D}(\boldsymbol{U}_{h_0})||^2_{L^2(\Omega_1)} + C_3^2||g_{\mathrm{N}}||^2_{L^2(\Gamma_{2\mathrm{N}})}\Big). \tag{5.10}$$

We obtain (5.5a) by recalling that $\boldsymbol{U}_{h_0} = \boldsymbol{U}^{h_0}$ and using Lemma 3 to bound $\boldsymbol{U}_{h_0}$ in (5.10).

Similarly for the stability of the Navier–Stokes velocity we choose $(\boldsymbol{v}_1, q_1) = (\boldsymbol{U}^*_{h_1}, P^*_{h_1})$ in (4.3a)-(4.3b) to obtain

$$\begin{aligned} a_{\mathrm{NS}}(\boldsymbol{U}^*_{h_1}, \boldsymbol{U}^*_{h_1}) + c_{\mathrm{NS}}(\boldsymbol{U}_{h_0}; \boldsymbol{U}^*_{h_1}, \boldsymbol{U}^*_{h_1}) + c_{\mathrm{NS}}(\boldsymbol{U}^*_{h_1}; \boldsymbol{U}_{h_0}, \boldsymbol{U}^*_{h_1}) + \frac{1}{G}\big(\boldsymbol{U}^*_{h_1}\cdot\boldsymbol{\tau}_{12}, \boldsymbol{U}^*_{h_1}\cdot\boldsymbol{\tau}_{12}\big)_{\Gamma_{12}} \\ = (\boldsymbol{f}_1, \boldsymbol{U}^*_{h_1})_{\Omega_1} + c_{\mathrm{NS}}(\boldsymbol{U}_{h_0}; \boldsymbol{U}_{h_0}, \boldsymbol{U}^*_{h_1}) - (\phi^*_{h_1}, \boldsymbol{U}^*_{h_1}\cdot\boldsymbol{n}_{12})_{\Gamma_{12}}. \end{aligned} \tag{5.11}$$

Using Lemma 1 and Young's inequality we bound the nonlinear terms in (5.11) as

$$\big|c_{\mathrm{NS}}(\boldsymbol{U}_{h_0}; \boldsymbol{U}^*_{h_1}, \boldsymbol{U}^*_{h_1}) + c_{\mathrm{NS}}(\boldsymbol{U}^*_{h_1}; \boldsymbol{U}^*_{h_0}, \boldsymbol{U}^*_{h_1})\big| \le C_4||\boldsymbol{D}(\boldsymbol{U}_{h_0})||_{L^2(\Omega_1)}||\boldsymbol{D}(\boldsymbol{U}^*_{h_1})||^2_{L^2(\Omega_1)}, \tag{5.12a}$$

$$\big|c_{\mathrm{NS}}(\boldsymbol{U}_{h_0}; \boldsymbol{U}_{h_0}, \boldsymbol{U}^*_{h_1})\big| \le \frac{3}{4\nu}C_4^2||\boldsymbol{D}(\boldsymbol{U}_{h_0})||^4_{L^2(\Omega_1)} + \frac{\nu}{3}||\boldsymbol{D}(\boldsymbol{U}^*_{h_1})||^2_{L^2(\Omega_1)}. \tag{5.12b}$$

Similarly using (5.1)-(5.2) we bound the rest of the terms in (5.11) as

$$\big|(\boldsymbol{f}_1, \boldsymbol{U}^*_{h_1})_{\Omega_1}\big| \le \frac{3}{4\nu}(\mathcal{P}_1C_1)^2||\boldsymbol{f}_1||^2_{L^2(\Omega_1)} + \frac{\nu}{3}||\boldsymbol{D}(\boldsymbol{U}^*_{h_1})||^2_{L^2(\Omega_1)} \tag{5.13a}$$

$$\big|(\phi^*_{h_1}, \boldsymbol{U}^*_{h_1}\cdot\boldsymbol{n}_{12})_{\Gamma_{12}}\big| \le \frac{3}{4\nu}(C_0C_1C_2)^2||\phi^*_{h_1}||^2_{\mathrm{DG}} + \frac{\nu}{3}||\boldsymbol{D}(\boldsymbol{U}^*_{h_1})||^2_{L^2(\Omega_1)}. \tag{5.13b}$$

Using Lemma 3 to bound $\boldsymbol{U}_{h_0}$ in (5.12a) and combining the bounds (5.12a)-(5.13b) in (5.11) yields

$$\Big(\nu - C_4\frac{\mathcal{R}}{\sqrt{2\nu}}\Big)||\boldsymbol{D}(\boldsymbol{U}^*_{h_1})||^2_{L^2(\Omega_1)} \le \frac{3}{4\nu}\Big((\mathcal{P}_1C_1)^2||\boldsymbol{f}_1||^2_{L^2(\Omega_1)} + C_4^2||\boldsymbol{D}(\boldsymbol{U}_{h_0})||^4_{L^2(\Omega_1)} + (C_0C_1C_2)^2||\phi^*_{h_1}||^2_{\mathrm{DG}}\Big) \tag{5.14}$$

Thus (5.5b) follows from the small data condition (5.4) and (5.5a) applied to (5.14).

The stability bounds for step 3 follow in the similar manner. Choosing $q_2 = \phi_{h_1}$ in (4.4) and bounding the resulting terms as in (5.9a)-(5.9c) yields

$$\frac{\kappa}{2}||\phi_{h_1}||^2_{\mathrm{DG}} \le \frac{3}{2\kappa}\Big(\mathcal{P}_2^2||f_2||^2_{L^2(\Omega_2)} + (C_0C_1C_2)^2||\boldsymbol{D}(\boldsymbol{U}^*_{h_1})||^2_{L^2(\Omega_1)} + C_3^2||g_{\mathrm{N}}||^2_{L^2(\Gamma_{2\mathrm{N}})}\Big). \tag{5.15}$$

Therefore (5.5c) follows by using (5.5b) to bound $\boldsymbol{U}^*_{h_1}$.

For the Navier-Stokes velocity bound we choose $(\boldsymbol{v}_1, q_1) = (\boldsymbol{U}_{h_1}, P_{h_1})$ in (4.5a)-(4.5b) yields

$$\begin{aligned} & a_{\mathrm{NS}}(\boldsymbol{U}_{h_1}, \boldsymbol{U}_{h_1}) + c_{\mathrm{NS}}(\boldsymbol{U}_{h_0}; \boldsymbol{U}_{h_1}, \boldsymbol{U}_{h_1}) + c_{\mathrm{NS}}(\boldsymbol{U}_{h_1}; \boldsymbol{U}_{h_0}, \boldsymbol{U}_{h_1}) + \frac{1}{G}\big(\boldsymbol{U}_{h_1} \cdot \boldsymbol{\tau}_{12}, \boldsymbol{U}_{h_1} \cdot \boldsymbol{\tau}_{12}\big)_{\Gamma_{12}} \\ = & (\boldsymbol{f}_1, \boldsymbol{U}_{h_1})_{\Omega_1} + c_{\mathrm{NS}}(\boldsymbol{U}_{h_0}; \boldsymbol{U}^*_{h_1}, \boldsymbol{U}_{h_1}) + c_{\mathrm{NS}}(\boldsymbol{U}^*_{h_1}; \boldsymbol{U}_{h_0} - \boldsymbol{U}^*_{h_1}, \boldsymbol{U}_{h_1}) - (\phi_{h_1}, \boldsymbol{U}_{h_1} \cdot \boldsymbol{n}_{12})_{\Gamma_{12}}. \end{aligned} \tag{5.16}$$

The nonlinear terms on the left hand side are treated as in (5.12a)-(5.12b). We bound the new nonlinear terms in the right-hand side of (5.16) as follows

$$\begin{aligned} & \left|c_{\mathrm{NS}}(\boldsymbol{U}_{h_0}; \boldsymbol{U}^*_{h_1}, \boldsymbol{U}_{h_1}) + c_{\mathrm{NS}}(\boldsymbol{U}^*_{h_1}; \boldsymbol{U}_{h_0} - \boldsymbol{U}^*_{h_1}, \boldsymbol{U}_{h_1})\right| \\ \leq \; & C_4 ||\boldsymbol{D}(\boldsymbol{U}^*_{h_1})||_{L^2(\Omega_1)} \Big\{ ||\boldsymbol{D}(\boldsymbol{U}_{h_0})||_{L^2(\Omega_1)} + ||\boldsymbol{D}(\boldsymbol{U}_{h_0} - \boldsymbol{U}^*_{h_1})||_{L^2(\Omega_1)} \Big\} ||\boldsymbol{D}(\boldsymbol{U}_{h_1})||_{L^2(\Omega_1)} \qquad (5.17) \\ \leq \; & \frac{3}{4\nu} \left[C_4 ||\boldsymbol{D}(\boldsymbol{U}^*_{h_1})||_{L^2(\Omega_1)} \Big\{ ||\boldsymbol{D}(\boldsymbol{U}_{h_0})||_{L^2(\Omega_1)} + ||\boldsymbol{D}(\boldsymbol{U}_{h_0} - \boldsymbol{U}^*_{h_1})||_{L^2(\Omega_1)} \Big\} \right]^2 + \frac{\nu}{3} ||\boldsymbol{D}(\boldsymbol{U}_{h_1})||^2_{L^2(\Omega_1)}. \end{aligned}$$

and treat the rest of the terms in (5.16) in a manner similar to (5.11) to obtain

$$\begin{aligned} & \left(\nu - C_4 \frac{\mathcal{R}}{\sqrt{2\nu}}\right) ||\boldsymbol{D}(\boldsymbol{U}_{h_1})||^2_{L^2(\Omega_1)} \leq \frac{3}{4\nu}\Bigg((\mathcal{P}_1 C_1)^2 ||\boldsymbol{f}_1||^2_{L^2(\Omega_1)} \qquad (5.18) \\ + \; & \left[C_4 ||\boldsymbol{D}(\boldsymbol{U}^*_{h_1})||_{L^2(\Omega_1)} \Big\{ ||\boldsymbol{D}(\boldsymbol{U}_{h_0})||_{L^2(\Omega_1)} + ||\boldsymbol{D}(\boldsymbol{U}_{h_0} - \boldsymbol{U}^*_{h_1})||_{L^2(\Omega_1)} \Big\} \right]^2 + (C_0 C_1 C_2)^2 ||\phi_{h_1}||^2_{\mathrm{DG}} \Bigg) \end{aligned}$$

The result (5.5d) follows from Lemma 3, (5.5b)-(5.5c) and the condition (5.4).

The proof the convergence results (5.6a)-(5.6b) and (5.7a)-(5.7b) are similar to the convergence of the two-grid method in [41, 53]. We refer the reader to [39] for a proof (5.6c) and (5.7c).

We proceed to the multilevel method. We begin by proving the stability and convergence of Step 2 of the decoupling scheme.

Theorem 5. *Under the assumptions of Lemma 4, the solution of stage 2 of the multilevel decoupled scheme* ($(J+1)-$ *level method*), (4.2), (4.3a)-(4.3b) *with* $j \geq 1$ *is stable*

$$\kappa ||\phi^*_{h_j}||^2_{\mathrm{DG}} \leq (\mathcal{D}^*_j)^2 \tag{5.19a}$$

$$2\nu ||\boldsymbol{D}(\boldsymbol{U}^*_{h_j})||^2_{L^2(\Omega_1)} \leq (\mathcal{N}^*_j)^2 \tag{5.19b}$$

where

$$\begin{aligned} \mathcal{D}^*_j &= \left[\frac{3}{\kappa}\left(\mathcal{P}_2^2 ||f_2||^2_{L^2(\Omega_2)} + (C_0C_1C_2)^2 \frac{\mathcal{N}^2_{j-1}}{2\nu} + C_3^2 ||g_{\mathrm{N}}||^2_{L^2(\Gamma_{2\mathrm{N}})}\right)\right]^{\frac{1}{2}}, \\ \mathcal{N}^*_j &= \left[\frac{3}{\nu}\left((\mathcal{P}_1 C_1)^2 ||\boldsymbol{f}_1||^2_{L^2(\Omega_1)} + C_4^2 \frac{\mathcal{N}^4_{j-1}}{4\nu^2} + (C_0C_1C_2)^2 \frac{(\mathcal{D}^*_j)^2}{\kappa}\right)\right]^{\frac{1}{2}}. \end{aligned}$$

Further, if the condition $h_j = h^2_{j-1}$ *holds then there exists a constant* C *independent of* h_j *such that*

$$||\phi - \phi^*_{h_j}||_{\mathrm{DG}} \leq C(h^2_{j-1} + h_j) \leq Ch_j, \tag{5.20a}$$

$$||\boldsymbol{D}(\boldsymbol{u} - \boldsymbol{U}^*_{h_j})||_{L^2(\Omega_1)} + ||p - P^*_{h_j}||_{L^2(\Omega_1)} \leq C(h^2_{j-1} + h_j) \leq Ch_j. \tag{5.20b}$$

$$||\boldsymbol{u} - \boldsymbol{U}^*_{h_j}||_{L^2(\Omega_1)} \leq C(h^3_{j-1} + h^2_j) \leq Ch_j^{\frac{3}{2}}. \tag{5.20c}$$

Proof. Theorem 5 will be proved by induction. First, we note that Lemma 4 shows that Theorem 5 is true for $j = 1$. We assume that Theorem 5 holds for $j = m$, with $1 \leq m \leq J-1$, specifically the following conditions hold

$$\kappa||\phi^*_{h_m}||_{\mathrm{DG}} \leq (\mathcal{D}^*_m)^2 \text{ and } \kappa||\phi_{h_m}||_{\mathrm{DG}} \leq (\mathcal{D}_m)^2, \tag{5.21a}$$

$$2\nu||\boldsymbol{D}(\boldsymbol{U}^*_{h_m})||^2_{L^2(\Omega_1)} \leq (\mathcal{N}^*_m)^2 \text{ and } 2\nu||\boldsymbol{D}(\boldsymbol{U}_{h_m})||^2_{L^2(\Omega_1)} \leq (\mathcal{N}_m)^2, \tag{5.21b}$$

under the condition

$$\nu^{\frac{3}{2}} > \sqrt{2}C_4\mathcal{N}_m \tag{5.22}$$

along with the convergence results (5.6a)-(5.7c) for $j = m$. We show that Theorem 5 holds for $j = m+1$.

We begin with the stability of the Darcy pressure by choosing $q_2 = \phi^*_{h_{m+1}}$ in (4.2) and using inequalities in (5.1)-(5.2) and Lemma 2 it follows that

$$\kappa||\phi^*_{h_{m+1}}||^2_{\mathrm{DG}} \leq \frac{3\mathcal{P}_2^2}{\kappa}||f_2||^2_{L^2(\Omega_2)} + \frac{3(C_0C_1C_2)^2}{\kappa}||\boldsymbol{D}(\boldsymbol{U}_{h_m})||^2_{L^2(\Omega_1)} + \frac{3C_3^2}{\kappa}||g_{\mathrm{N}}||^2_{L^2(\Gamma_{2\mathrm{N}})}. \tag{5.23}$$

Therefore the Darcy pressure bound (5.19a) follows for $j = m+1$ from the induction assumption (5.21b) applied to (5.23). Similarly, by selecting $(\boldsymbol{v}_1, q_1) = (\boldsymbol{U}^*_{h_{m+1}}, P^*_{h_{m+1}})$ in (4.3a)-(4.3b) we obtain

$$\begin{aligned}&\left(\nu - C_4\frac{\mathcal{N}_m}{\sqrt{2\nu}}\right)||\boldsymbol{D}(\boldsymbol{U}^*_{h_{m+1}})||^2_{L^2(\Omega_1)} \leq \\ &\frac{3}{4\nu}\left((\mathcal{P}_1C_1)^2||\boldsymbol{f}_1||^2_{L^2(\Omega_1)} + C_4^2||\boldsymbol{D}(\boldsymbol{U}_{h_m})||^4_{L^2(\Omega_1)} + (C_0C_1C_2)^2||\phi^*_{h_{m+1}}||^2_{\mathrm{DG}}\right)\end{aligned} \tag{5.24}$$

Thus the velocity bound (5.19b) follows for $j = m+1$ from applying (5.19a) and (5.21b) to (5.24).

For the error analysis, we first recall that from the definition of the trilinear form it is easy to verify that if $(\boldsymbol{U}^{h_{m+1}}, \boldsymbol{U}_{h_m}, \boldsymbol{v}_1) \in [H^1(\Omega_1)]^3$ then the following identity holds; see e.g. [42]

$$\begin{aligned}c_{\mathrm{NS}}(\boldsymbol{U}^{h_{m+1}}; U^{h_{m+1}}, \boldsymbol{v}_1) &= c_{\mathrm{NS}}(\boldsymbol{U}_{h_m}; \boldsymbol{U}^{h_{m+1}}, \boldsymbol{v}_1) + c_{\mathrm{NS}}(\boldsymbol{U}^{h_{m+1}}; \boldsymbol{U}_{h_m}, \boldsymbol{v}_1)\\ &-c_{\mathrm{NS}}(\boldsymbol{U}_{h_m}; \boldsymbol{U}_{h_m}, \boldsymbol{v}_1) + c_{\mathrm{NS}}(\boldsymbol{U}^{h_{m+1}} - \boldsymbol{U}_{h_m}; \boldsymbol{U}^{h_{m+1}} - \boldsymbol{U}_{h_m}, \boldsymbol{v}_1),\end{aligned} \tag{5.25}$$

where $\boldsymbol{U}^{h_{m+1}}$ and $\boldsymbol{U}_{h_m}$ are the solutions from the fully coupled scheme at mesh level $m+1$ and multilevel method at mesh level m, respectively. We replace the nonlinear term in the fully coupled problem (3.5a)-(3.5b) using the identity (5.25) and take the difference with the decoupled problems (4.2) ,(4.3a)-(4.3b) to obtain

$$\begin{aligned}&\forall \boldsymbol{v}_1 \in \boldsymbol{X}_1^{h_{m+1}}, \forall q_1 \in M_1^{h_{m+1}}, q_2 \in M_2^{h_{m+1}},\\ &a_{\mathrm{NS}}\big(\boldsymbol{U}^{h_{m+1}} - \boldsymbol{U}^*_{h_{m+1}}, \boldsymbol{v}_1\big) + b_{\mathrm{NS}}\big(\boldsymbol{v}_1, P^{h_{m+1}} - P^*_{h_{m+1}}\big) + c_{\mathrm{NS}}\big(\boldsymbol{U}_{h_m}; \boldsymbol{U}^{h_{m+1}} - \boldsymbol{U}^*_{h_{m+1}}, \boldsymbol{v}_1\big)\\ &\quad + c_{\mathrm{NS}}\big(\boldsymbol{U}^{h_{m+1}} - \boldsymbol{U}^*_{h_{m+1}}; \boldsymbol{U}_{h_m}, \boldsymbol{v}_1\big) + a_{\mathrm{D}}(\phi^{h_{m+1}} - \phi^*_{h_{m+1}}, q_2)\\ &\quad + \frac{1}{G}\big((\boldsymbol{U}^{h_{m+1}} - \boldsymbol{U}^*_{h_{m+1}}) \cdot \boldsymbol{\tau}_{12}, \boldsymbol{v}_1 \cdot \boldsymbol{\tau}_{12}\big)_{\Gamma_{12}} = \big(\phi^*_{h_{m+1}} - \phi^{h_{m+1}}, \boldsymbol{v}_1 \cdot \boldsymbol{n}_{12}\big)_{\Gamma_{12}}\\ &\quad + \big((\boldsymbol{U}^{h_{m+1}} - \boldsymbol{U}_{h_m}) \cdot \boldsymbol{n}_{12}, q_2\big)_{\Gamma_{12}} - c_{\mathrm{NS}}\big(\boldsymbol{U}^{h_{m+1}} - \boldsymbol{U}_{h_m}; \boldsymbol{U}^{h_{m+1}} - \boldsymbol{U}_{h_m}, \boldsymbol{v}_1\big)\end{aligned} \tag{5.26a}$$

$$\forall q_1 \in M_1^h, \quad b_{\mathrm{NS}}\big(\boldsymbol{U}^*_{h_{m+1}} - \boldsymbol{U}^{h_{m+1}}, q_1\big) = 0. \tag{5.26b}$$

Setting $(\boldsymbol{v}_1, q_1) = \boldsymbol{0}$ and $q_2 = \phi^{h_{m+1}} - \phi^*_{h_{m+1}}$ in (5.26a)-(5.26b), it follows from arguments similar to the analysis of the multilevel Stokes/Darcy method in [9] that

$$||\phi^{h_{m+1}} - \phi^*_{h_{m+1}}||_{\mathrm{DG}} \leq C\big\{h_m||\boldsymbol{D}(\boldsymbol{U}^{h_{m+1}} - \boldsymbol{U}_{h_m})||_{L^2(\Omega_1)} + ||\boldsymbol{U}^{h_{m+1}} - \boldsymbol{U}_{h_m}||_{L^2(\Omega_1)}\big\} \tag{5.27a}$$

$$\leq C\big\{h_m(h_{m+1} + h_m) + h_{m+1}^2 + h_m^2\big\} \leq Ch_m^2, \tag{5.27b}$$

Here, (5.27b) is obtained by applying the triangular inequality to each error term in (5.27a) and applying Lemma 3, the induction hypothesis ((5.7b)-(5.7c) for $j = m$) and dropping high order terms.

For the velocity error we proceed by choosing $\boldsymbol{v}_1 = \boldsymbol{U}^{h_{m+1}} - \boldsymbol{U}^*_{h_{m+1}}$, $q_1 = P^{h_{m+1}} - P^*_{h_{m+1}}$ and $q_2 = 0$ in (5.26a)-(5.26b) yielding

$$2\nu||\boldsymbol{D}(\boldsymbol{U}^{h_{m+1}} - \boldsymbol{U}^*_{h_{m+1}})||^2_{L^2(\Omega_1)} \leq |N_1| + |N_\Gamma| + |N_2|, \tag{5.28}$$

where

$$\begin{aligned} N_1 &= c_{\mathrm{NS}}\big(\boldsymbol{U}_{h_m}; \boldsymbol{U}^{h_{m+1}} - \boldsymbol{U}^*_{h_{m+1}}, \boldsymbol{U}^{h_{m+1}} - \boldsymbol{U}^*_{h_{m+1}}\big) + c_{\mathrm{NS}}\big(\boldsymbol{U}^{h_{m+1}} - \boldsymbol{U}^*_{h_{m+1}}; \boldsymbol{U}_{h_m}, \boldsymbol{U}^{h_{m+1}} - \boldsymbol{U}^*_{h_{m+1}}\big), \\ N_2 &= c_{\mathrm{NS}}\big(\boldsymbol{U}^{h_{m+1}} - \boldsymbol{U}_{h_m}; \boldsymbol{U}^{h_{m+1}} - \boldsymbol{U}_{h_m}, \boldsymbol{U}^{h_{m+1}} - \boldsymbol{U}^*_{h_{m+1}}\big), \\ N_\Gamma &= \big(\phi^*_{h_{m+1}} - \phi^{h_{m+1}}, (\boldsymbol{U}^{h_{m+1}} - \boldsymbol{U}^*_{h_{m+1}}) \cdot \boldsymbol{n}_{12}\big)_{\Gamma_{12}}. \end{aligned}$$

Applying Lemma 1 and the induction hypothesis ((5.21b) for $j = m$) it follows that

$$\begin{aligned} |N_1| &\leq C_4||\boldsymbol{D}(\boldsymbol{U}_{h_m})||_{L_2(\Omega_1)}||\boldsymbol{D}(\boldsymbol{U}^{h_{m+1}} - \boldsymbol{U}^*_{h_{m+1}})||^2_{L^2(\Omega_1)} \\ &\leq C_4\frac{\mathcal{N}_m}{\sqrt{2\nu}}||\boldsymbol{D}(\boldsymbol{U}^{h_{m+1}} - \boldsymbol{U}^*_{h_{m+1}})||^2_{L^2(\Omega_1)}. \end{aligned} \tag{5.29}$$

Similarly using Lemma 1, Young's inequality and inequalities in (5.1)-(5.2) we can bound

$$|N_2| \leq \frac{C_4^2}{2\nu}||\boldsymbol{D}(\boldsymbol{U}^{h_{m+1}} - \boldsymbol{U}_{h_m})||^4_{L^2(\Omega_1)} + \frac{\nu}{2}||\boldsymbol{D}(\boldsymbol{U}^{h_{m+1}} - \boldsymbol{U}^*_{h_{m+1}})||^2_{L^2(\Omega_1)} \tag{5.30a}$$

$$|N_\Gamma| \leq \frac{(C_0C_1C_2)^2}{2\nu}||\phi^*_{h_{m+1}} - \phi^{h_{m+1}}||^2_{\mathrm{DG}} + \frac{\nu}{2}||\boldsymbol{D}(\boldsymbol{U}^{h_{m+1}} - \boldsymbol{U}^*_{h_{m+1}})||^2_{L^2(\Omega_1)}. \tag{5.30b}$$

Combining (5.29)-(5.30b) in (5.28) yields

$$\left(\nu - C_4\frac{\mathcal{N}_m}{\sqrt{2\nu}}\right)||\boldsymbol{D}(\boldsymbol{U}^{h_{m+1}} - \boldsymbol{U}^*_{h_{m+1}})||^2_{L^2(\Omega_1)} \leq \frac{C_4^2}{2\nu}||\boldsymbol{D}(\boldsymbol{U}^{h_{m+1}} - \boldsymbol{U}_{h_m})||^4_{L^2(\Omega_1)} + \frac{(C_0C_1C_2)^2}{2\nu}||\phi^*_{h_{m+1}} - \phi^{h_{m+1}}||^2_{\mathrm{DG}}, \tag{5.31}$$

then applying (5.22) to (5.31) we obtain

$$||\boldsymbol{D}(\boldsymbol{U}^{h_{m+1}} - \boldsymbol{U}^*_{h_{m+1}})||^2_{L^2(\Omega_1)} \leq \frac{C_4^2}{4\nu^2}||\boldsymbol{D}(\boldsymbol{U}^{h_{m+1}} - \boldsymbol{U}_{h_m})||^4_{L^2(\Omega_1)} + \frac{(C_0C_1C_2)^2}{4\nu^2}||\phi^*_{h_{m+1}} - \phi^{h_{m+1}}||^2_{\mathrm{DG}}. \tag{5.32}$$

The first term in (5.32) can be bound by applying Lemma 3 and the induction hypothesis ((5.7b) for $j = m$) as follows

$$||\boldsymbol{D}(\boldsymbol{U}^{h_{m+1}} - \boldsymbol{U}_{h_m})||_{L^2(\Omega_1)} \leq ||\boldsymbol{D}(\boldsymbol{U}^{h_{m+1}} - \boldsymbol{u})||_{L^2(\Omega_1)} + ||\boldsymbol{D}(\boldsymbol{u} - \boldsymbol{U}_{h_m})||_{L^2(\Omega_1)} \leq C(h_{m+1} + h_m). \tag{5.33}$$

The bound for the second term in (5.32) follows from (5.27b), therefore we can conclude that

$$||\boldsymbol{D}(\boldsymbol{U}^{h_{m+1}} - \boldsymbol{U}^*_{h_{m+1}})||^2_{L^2(\Omega_1)} \leq Ch_m^4 \tag{5.34}$$

after dropping higher order terms.

The pressure error bound can be derived using standard inf-sup arguments. We include the proof for completeness. Setting $q_2 = 0$ in (5.26a) yields

$$\begin{aligned} &a_{\mathrm{NS}}\big(\boldsymbol{U}^{h_{m+1}} - \boldsymbol{U}^*_{h_{m+1}}, \boldsymbol{v}_1\big) + b_{\mathrm{NS}}\big(\boldsymbol{v}_1, P^{h_{m+1}} - P^*_{h_{m+1}}\big) + c_{\mathrm{NS}}\big(\boldsymbol{U}_{h_m}; \boldsymbol{U}^{h_{m+1}} - \boldsymbol{U}^*_{h_{m+1}}, \boldsymbol{v}_1\big) \\ &+c_{\mathrm{NS}}\big(\boldsymbol{U}^{h_{m+1}} - \boldsymbol{U}^*_{h_{m+1}}; \boldsymbol{U}_{h_m}, \boldsymbol{v}_1\big) + \frac{1}{G}\big((\boldsymbol{U}^{h_{m+1}} - \boldsymbol{U}^*_{h_{m+1}}) \cdot \boldsymbol{\tau}_{12}, \boldsymbol{v}_1 \cdot \boldsymbol{\tau}_{12}\big)_{\Gamma_{12}} \\ &= \big(\phi^*_{h_{m+1}} - \phi^{h_{m+1}}, \boldsymbol{v}_1 \cdot \boldsymbol{n}_{12}\big)_{\Gamma_{12}} - c_{\mathrm{NS}}\big(\boldsymbol{U}^{h_{m+1}} - \boldsymbol{U}_{h_m}; \boldsymbol{U}^{h_{m+1}} - \boldsymbol{U}_{h_m}, \boldsymbol{v}_1\big). \end{aligned} \tag{5.35}$$

For brevity, we define

$$
\begin{aligned}
T_1 &= c_{\rm NS}\big(\boldsymbol{U}_{h_m};\boldsymbol{U}^{h_{m+1}}-\boldsymbol{U}^*_{h_{m+1}},\boldsymbol{v}_1\big)+c_{\rm NS}\big(\boldsymbol{U}^{h_{m+1}}-\boldsymbol{U}^*_{h_{m+1}};\boldsymbol{U}_{h_m},\boldsymbol{v}_1\big),\\
T_\Gamma &= \big(\phi^*_{h_{m+1}}-\phi^{h_{m+1}},\boldsymbol{v}_1\cdot\boldsymbol{n}_{12}\big)_{\Gamma_{12}}-\frac{1}{G}\big((\boldsymbol{U}^{h_{m+1}}-\boldsymbol{U}^*_{h_{m+1}})\cdot\boldsymbol{\tau}_{12},\boldsymbol{v}_1\cdot\boldsymbol{\tau}_{12}\big)_{\Gamma_{12}},\\
T_2 &= c_{\rm NS}\big(\boldsymbol{U}^{h_{m+1}}-\boldsymbol{U}_{h_m};\boldsymbol{U}^{h_{m+1}}-\boldsymbol{U}_{h_m},\boldsymbol{v}_1\big).
\end{aligned}
$$

These terms can be bound using Lemma 1, (5.21b) and inequalities in (5.1)-(5.2) as follows

$$
\begin{aligned}
|T_1| &\le C_4\frac{\mathcal{N}_m}{\sqrt{2\nu}}||\boldsymbol{D}(\boldsymbol{U}^{h_{m+1}}-\boldsymbol{U}^*_{h_{m+1}})||_{L^2(\Omega_1)}||\boldsymbol{D}(\boldsymbol{v}_1)||_{L^2(\Omega_1)}, && (5.36a)\\
|T_\Gamma| &\le C_0C_1\left(C_2||\phi^*_{h_{m+1}}-\phi^{h_{m+1}}||_{\rm DG}+\frac{1}{G}||\boldsymbol{D}(\boldsymbol{U}^{h_{m+1}}-\boldsymbol{U}^*_{h_{m+1}})||_{L^2(\Omega_1)}\right)||\boldsymbol{D}(\boldsymbol{v}_1)||_{L^2(\Omega_1)}, && (5.36b)\\
|T_2| &\le C_4||\boldsymbol{D}(\boldsymbol{U}^{h_{m+1}}-\boldsymbol{U}_{h_m})||^2_{L^2(\Omega_1)}||\boldsymbol{D}(\boldsymbol{v}_1)||_{L^2(\Omega_1)}. && (5.36c)
\end{aligned}
$$

Applying the inf-sup condition (3.1) to (5.35) we obtain

$$
\begin{aligned}
||P^{h_{m+1}}-P^*_{h_{m+1}}||_{L^2(\Omega_1)} &\le \frac{b_{\rm NS}(\boldsymbol{v}_1,P^{h_{m+1}}-P^*_{h_{m+1}})}{||\boldsymbol{D}(\boldsymbol{v}_1)||_{L^2(\Omega_1)}}\\
&\le \frac{|a_{\rm NS}(\boldsymbol{U}^{h_{m+1}}-\boldsymbol{U}^*_{h_{m+1}},\boldsymbol{v}_1)|+|T_1|+|T_\Gamma|+|T_2|}{||\boldsymbol{D}(\boldsymbol{v}_1)||_{L^2(\Omega_1)}}. \qquad (5.37)
\end{aligned}
$$

Then using the error estimates (5.27b) and (5.33)-(5.34) in the bounds (5.36a)-(5.36c) and using Cauchy–Schwarz inequality to bound $a_{\rm NS}$ in (5.37) yields

$$
\begin{aligned}
||P^{h_{m+1}}-P^*_{h_{m+1}}||_{L^2(\Omega_1)} &\le \left(2\nu+C_4\frac{\mathcal{N}_m}{\sqrt{2\nu}}+\frac{C_0C_1}{G}\right)||\boldsymbol{D}(\boldsymbol{U}^{h_{m+1}}-\boldsymbol{U}^*_{h_{m+1}})||_{L^2(\Omega_1)}\\
&+ C_4||\boldsymbol{D}(\boldsymbol{U}^{h_{m+1}}-\boldsymbol{U}_{h_m})||^2_{L^2(\Omega_1)}+C_0C_1C_2||\phi^*_{h_{m+1}}-\phi^{h_{m+1}}||_{\rm DG}\\
&\le Ch_m^2. \qquad (5.38)
\end{aligned}
$$

The convergence results (5.20a)-(5.20b) follow from the triangular inequalities,

$$
\begin{aligned}
||\phi-\phi^*_{h_{m+1}}||_{\rm DG} &\le ||\phi-\phi^{h_{m+1}}||_{\rm DG}+||\phi^{h_{m+1}}-\phi^*_{h_{m+1}}||_{\rm DG},\\
||\boldsymbol{D}(\boldsymbol{u}-\boldsymbol{U}^*_{h_{m+1}})||_{L^2(\Omega_1)} &\le ||\boldsymbol{D}(\boldsymbol{u}-\boldsymbol{U}^{h_{m+1}})||_{L^2(\Omega_1)}+||\boldsymbol{D}(\boldsymbol{U}^{h_{m+1}}-\boldsymbol{U}^*_{h_{m+1}})||_{L^2(\Omega_1)},\\
||p-P^*_{h_{m+1}}||_{L^2(\Omega_1)} &\le ||p-P^{h_{m+1}}||_{L^2(\Omega_1)}+||P^{h_{m+1}}-P^*_{h_{m+1}}||_{L^2(\Omega_1)},
\end{aligned}
$$

(5.27b), (5.34), (5.38), Lemma 3 and the mesh relation $h_{m+1}=h_m^2$.

We conclude by proving the L_2 error bound for the velocity for $j=m+1$, the proof follows from the arguments similar for the two-grid method in [39]. We consider the following linearized adjoint problem

$$
\begin{gathered}
\text{Find } (\boldsymbol{w}^*,r^*)\in(\boldsymbol{X}_1,M_1) \text{ s.t. } \forall\boldsymbol{v}_1\in\boldsymbol{X}_1,\forall q_1\in M_1,\\
a_{\rm NS}(\boldsymbol{v}_1,\boldsymbol{w}^*)+b_{\rm NS}(\boldsymbol{v}_1,r^*)+b_{\rm NS}(\boldsymbol{w}^*,q_1)+c_{\rm NS}(\boldsymbol{u};\boldsymbol{v}_1,\boldsymbol{w}^*)+c_{\rm NS}(\boldsymbol{v}_1;\boldsymbol{u},\boldsymbol{w}^*)\\
+\frac{1}{G}\big(\boldsymbol{v}_1\cdot\boldsymbol{\tau}_{12},\boldsymbol{w}^*\cdot\boldsymbol{\tau}_{12}\big)_{\Gamma_{12}}+(\phi-\phi^*_{h_{m+1}},\boldsymbol{w}^*\cdot\boldsymbol{n}_{12})_{\Gamma_{12}}=(\boldsymbol{g}_1^*,\boldsymbol{v}_1)_{\Omega_1}.
\end{gathered}
\qquad (5.39)
$$

where $(\boldsymbol{u},\phi)$ is a nonsingular solution of (2.4a)-(2.4b). We assume that the problem (5.39) is $H^2(\Omega_1)$ regular so that for any $\boldsymbol{g}_1^*\in L^2(\Omega_1)$ the solution $(\boldsymbol{w}^*,r^*)\in H^2(\Omega_1)\times H^1(\Omega_1)$ satisfies the H^2-regularity assumption

$$
||\boldsymbol{w}^*||_{H^2(\Omega_1)}+||r^*||_{H^1(\Omega_1)}\le C||\boldsymbol{g}_1^*||_{L^2(\Omega_1)}. \qquad (5.40)
$$

Setting $\boldsymbol{g}_1^* = \boldsymbol{u} - \boldsymbol{U}^*_{h_{m+1}}$ and $(\boldsymbol{v}_1, q_1) = (\boldsymbol{u} - \boldsymbol{U}^*_{h_{m+1}}, p - P^*_{h_{m+1}})$ in (5.39) and splitting the nonlinear terms, we obtain

$$\begin{aligned}
||\boldsymbol{u} - \boldsymbol{U}^*_{h_{m+1}}||^2_{L^2(\Omega_1)} &= a_{\rm NS}(\boldsymbol{u} - \boldsymbol{U}^*_{h_{m+1}}, \boldsymbol{w}^*) + b_{\rm NS}(\boldsymbol{u} - \boldsymbol{U}^*_{h_{m+1}}, r^*) + b_{\rm NS}(\boldsymbol{w}^*, p - P^*_{h_{m+1}}) \\
&+ c_{\rm NS}(\boldsymbol{U}_{h_m}; \boldsymbol{u} - \boldsymbol{U}^*_{h_{m+1}}, \boldsymbol{w}^*) + c_{\rm NS}(\boldsymbol{u} - \boldsymbol{U}^*_{h_{m+1}}; \boldsymbol{U}_{h_m}, \boldsymbol{w}^*) \\
&+ \frac{1}{G}((\boldsymbol{u} - \boldsymbol{U}^*_{h_{m+1}}) \cdot \boldsymbol{\tau}_{12}, \boldsymbol{w}^* \cdot \boldsymbol{\tau}_{12})_{\Gamma_{12}} + (\phi - \phi^*_{h_{m+1}}, \boldsymbol{w}^* \cdot \boldsymbol{n}_{12})_{\Gamma_{12}} \\
&+ c_{\rm NS}(\boldsymbol{u} - \boldsymbol{U}_{h_m}; \boldsymbol{u} - \boldsymbol{U}^*_{h_{m+1}}, \boldsymbol{w}^*) + c_{\rm NS}(\boldsymbol{u} - \boldsymbol{U}^*_{h_{m+1}}; \boldsymbol{u} - \boldsymbol{U}_{h_m}, \boldsymbol{w}^*). \qquad (5.41)
\end{aligned}$$

Setting $q_2 = 0$ in (2.4a)-(2.4b) and subtracting Step 2 of the multilevel method, (4.3a)-(4.3b) yields

$$\begin{aligned}
&a_{\rm NS}(\boldsymbol{u} - \boldsymbol{U}^*_{h_{m+1}}, \boldsymbol{v}_1) + b_{\rm NS}(\boldsymbol{u} - \boldsymbol{U}^*_{h_{m+1}}, q_1) + b_{\rm NS}(\boldsymbol{v}_1, p - P^*_{h_{m+1}}) + c_{\rm NS}(\boldsymbol{U}_{h_m}; \boldsymbol{u} - \boldsymbol{U}^*_{h_{m+1}}, \boldsymbol{v}_1) \\
&+ c_{\rm NS}(\boldsymbol{u} - \boldsymbol{U}^*_{h_{m+1}}; \boldsymbol{U}_{h_m}, \boldsymbol{v}_1) + \frac{1}{G}\big((\boldsymbol{u} - \boldsymbol{U}^*_{h_{m+1}}) \cdot \boldsymbol{\tau}_{12}, \boldsymbol{v}_1 \cdot \boldsymbol{\tau}_{12}\big)_{\Gamma_{12}} + (\phi - \phi^*_{h_{m+1}}, \boldsymbol{v}_1 \cdot \boldsymbol{n}_{12})_{\Gamma_{12}} \qquad (5.42) \\
&+ c_{\rm NS}(\boldsymbol{u} - \boldsymbol{U}_{h_m}; \boldsymbol{u} - \boldsymbol{U}_{h_m}, \boldsymbol{v}_1) = 0.
\end{aligned}$$

We subtract the error term (5.42) from the right hand side of (5.41) to obtain

$$\begin{aligned}
||\boldsymbol{u} - \boldsymbol{U}^*_{h_{m+1}}||^2_{L^2(\Omega_1)} &= a_{\rm NS}(\boldsymbol{u} - \boldsymbol{U}^*_{h_{m+1}}, \boldsymbol{w}^* - \boldsymbol{v}_1) + b_{\rm NS}(\boldsymbol{u} - \boldsymbol{U}^*_{h_{m+1}}, r^* - q_1) \\
&+ b_{\rm NS}(\boldsymbol{w}^* - \boldsymbol{v}_1, p - P^*_{h_{m+1}}) + c_{\rm NS}(\boldsymbol{U}_{h_m}; \boldsymbol{u} - \boldsymbol{U}^*_{h_{m+1}}, \boldsymbol{w}^* - \boldsymbol{v}_1) \\
&+ c_{\rm NS}(\boldsymbol{u} - \boldsymbol{U}^*_{h_{m+1}}; \boldsymbol{U}_{h_m}, \boldsymbol{w}^* - \boldsymbol{v}_1) + (\phi - \phi^*_{h_{m+1}}, (\boldsymbol{w}^* - \boldsymbol{v}_1) \cdot \boldsymbol{n}_{12})_{\Gamma_{12}} \qquad (5.43) \\
&+ \frac{1}{G}\big((\boldsymbol{u} - \boldsymbol{U}^*_{h_{m+1}}) \cdot \boldsymbol{\tau}_{12}, (\boldsymbol{w}^* - \boldsymbol{v}_1) \cdot \boldsymbol{\tau}_{12}\big)_{\Gamma_{12}} + c_{\rm NS}(\boldsymbol{u} - \boldsymbol{U}_{h_m}; \boldsymbol{u} - \boldsymbol{U}^*_{h_{m+1}}, \boldsymbol{w}^*) \\
&+ c_{\rm NS}(\boldsymbol{u} - \boldsymbol{U}^*_{h_{m+1}}; \boldsymbol{u} - \boldsymbol{U}_{h_m}, \boldsymbol{w}^*) - c_{\rm NS}(\boldsymbol{u} - \boldsymbol{U}_{h_m}; \boldsymbol{u} - \boldsymbol{U}_{h_m}, \boldsymbol{v}_1).
\end{aligned}$$

We bound the first three terms of the right hand of (5.43) using (5.1), (5.20b) and (5.40) and as follows

$$\begin{aligned}
a_{\rm NS}(\boldsymbol{u} - \boldsymbol{U}^*_{h_{m+1}}, \boldsymbol{w}^* - \boldsymbol{v}_1) &\le ||\boldsymbol{D}(\boldsymbol{u} - \boldsymbol{U}^*_{h_{m+1}})||_{L^2(\Omega_1)} ||\boldsymbol{D}(\boldsymbol{w}^* - \boldsymbol{v}_1)||_{L^2(\Omega_1)} \\
&\le C(h_m^2 + h_{m+1}) h_{m+1} ||\boldsymbol{g}_1^*||_{L^2(\Omega_1)}, \qquad (5.44a) \\
b_{\rm NS}(\boldsymbol{u} - \boldsymbol{U}^*_{h_{m+1}}, r^* - q_1) &\le C_0 C_1 ||\boldsymbol{D}(\boldsymbol{u} - \boldsymbol{U}^*_{h_{m+1}})||_{L^2(\Omega_1)} ||r^* - q_1||_{L^2(\Omega_1)} \\
&\le C(h_m^2 + h_{m+1}) h_{m+1} ||\boldsymbol{g}_1^*||_{L^2(\Omega_1)}, \qquad (5.44b) \\
b_{\rm NS}(\boldsymbol{w}^* - \boldsymbol{v}_1, p - P^*_{h_{m+1}}) &\le C_0 C_1 ||\boldsymbol{D}(\boldsymbol{w}^* - \boldsymbol{v}_1)||_{L^2(\Omega_1)} ||p - P^*_{h_{m+1}}||_{L^2(\Omega_1)} \\
&\le C h_{m+1} ||\boldsymbol{g}_1^*||_{L^2(\Omega_1)} (h_m^2 + h_{m+1}). \qquad (5.44c)
\end{aligned}$$

Similarly for the interface terms, using (5.1)-(5.2), from the newly derived estimates (5.20a)-(5.20b) and (5.40) we have

$$\begin{aligned}
&\Big|(\phi - \phi^*_{h_{m+1}}, (\boldsymbol{w}^* - \boldsymbol{v}_1) \cdot \boldsymbol{n}_{12})_{\Gamma_{12}} + \frac{1}{G}\big((\boldsymbol{u} - \boldsymbol{U}^*_{h_{m+1}}) \cdot \boldsymbol{\tau}_{12}, (\boldsymbol{w}^* - \boldsymbol{v}_1) \cdot \boldsymbol{\tau}_{12}\big)_{\Gamma_{12}}\Big| \\
&\le \big(C_2 ||\phi - \phi^*_{h_{m+1}}||_{\rm DG} + \frac{C_0 C_1}{G} ||\boldsymbol{D}(\boldsymbol{u} - \boldsymbol{U}^*_{h_{m+1}})||_{L^2(\Omega_1)}\big) C_0 C_1 ||\boldsymbol{D}(\boldsymbol{w}^* - \boldsymbol{v}_1)||_{L^2(\Omega_1)} \\
&\le C(h_m^2 + h_{m+1}) h_{m+1} ||\boldsymbol{g}_1^*||_{L^2(\Omega_1)}). \qquad (5.45)
\end{aligned}$$

The rest of the terms are bound using Lemma 1, (5.20a)-(5.20b) and the stability and convergence assumptions of the induction hypothesis ((5.21b),(5.7b)-(5.7c) for $j = m$) and (5.40) in the following manner

$$\begin{aligned}
\big|c_{\mathrm{NS}}(\boldsymbol{U}_{h_m};\boldsymbol{u}-\boldsymbol{U}^*_{h_{m+1}},\boldsymbol{w}^*-\boldsymbol{v}_1) &+ c_{\mathrm{NS}}(\boldsymbol{u}-\boldsymbol{U}^*_{h_{m+1}};\boldsymbol{U}_{h_m},\boldsymbol{w}^*-\boldsymbol{v}_1)\big| \\
&\le C_4||\boldsymbol{D}(\boldsymbol{U}_{h_m})||_{L^2(\Omega_1)}||\boldsymbol{D}(\boldsymbol{u}-\boldsymbol{U}^*_{h_{m+1}})||_{L^2(\Omega_1)}||\boldsymbol{D}(\boldsymbol{w}^*-\boldsymbol{v}_1)||_{L^2(\Omega_1)} \\
&\le C(h_m^2+h_{m+1})h_{m+1}||\boldsymbol{g}_1^*||_{L^2(\Omega_1)}, &\text{(5.46a)} \\
\big|c_{\mathrm{NS}}(\boldsymbol{u}-\boldsymbol{U}_{h_m};\boldsymbol{u}-\boldsymbol{U}^*_{h_{m+1}},\boldsymbol{w}^*) &+ c_{\mathrm{NS}}(\boldsymbol{u}-\boldsymbol{U}^*_{h_{m+1}};\boldsymbol{u}-\boldsymbol{U}_{h_m},\boldsymbol{w}^*)\big| \\
&\le C_4||\boldsymbol{u}-\boldsymbol{U}_{h_m}||_{L^2(\Omega_1)}||\boldsymbol{D}(\boldsymbol{u}-\boldsymbol{U}^*_{h_{m+1}})||_{L^2(\Omega_1)}||\boldsymbol{w}^*||_{H^2(\Omega_1)} \\
&\le Ch_m^2(h_m^2+h_{m+1})||\boldsymbol{g}_1^*||_{L^2(\Omega_1)}, &\text{(5.46b)} \\
\big|c_{\mathrm{NS}}(\boldsymbol{u}-\boldsymbol{U}_{h_m};\boldsymbol{u}-\boldsymbol{U}_{h_m},\boldsymbol{v}_1)\big| &\le \big|c_{\mathrm{NS}}(\boldsymbol{u}-\boldsymbol{U}_{h_m};\boldsymbol{u}-\boldsymbol{U}_{h_m},\boldsymbol{w}^*-\boldsymbol{v}_1)+c_{\mathrm{NS}}(\boldsymbol{u}-\boldsymbol{U}_{h_m};\boldsymbol{u}-\boldsymbol{U}_{h_m},\boldsymbol{w}^*)\big| \\
&\le C_4\big(||\boldsymbol{D}(\boldsymbol{u}-\boldsymbol{U}_{h_m})||^2_{L^2(\Omega_1)}||\boldsymbol{D}(\boldsymbol{w}^*-\boldsymbol{v}_1)||_{L^2(\Omega_1)} \\
&+ ||\boldsymbol{D}(\boldsymbol{u}-\boldsymbol{U}_{h_m})||_{L^2(\Omega_1)}||\boldsymbol{u}-\boldsymbol{U}_{h_m}||_{L^2(\Omega_1)}||\boldsymbol{w}^*||_{H^2(\Omega_1)}\big) \\
&\le C(h_m^2h_{m+1}+h_m^3))||\boldsymbol{g}_1^*||_{L^2(\Omega_1)}). &\text{(5.46c)}
\end{aligned}$$

Combining (5.44a)-(5.46c) and dropping higher order terms yields

$$||\boldsymbol{u}-\boldsymbol{U}^*_{h_{m+1}}||^2_{L^2(\Omega_1)} \le C(h_m^3+h_{m+1}^2)||\boldsymbol{g}_1^*||_{L^2(\Omega_1)}.$$

The result (5.20c) follows from the mesh relation $h_{m+1} = h_m^2$ and recalling that $\boldsymbol{g}_1^* = \boldsymbol{u}-\boldsymbol{U}^*_{h_{m+1}}$.

Remark 2. The L_2 error convergence rate for the free flow velocity in Theorem 5 is suboptimal for $h_j = h_{j-1}^2$. However, our numerical experiments seem to indicate that that the convergence is optimal therefore a finer analysis may be needed. In this work, the addition of the correction step allows us to prove optimal convergence of the final Navier–Stokes velocity solution in the L_2 norm with mesh spacing $h_j = h_{j-1}^2$. Our numerical results show that the correction step is necessary to improve the quality of the decoupled solution most notably in the porous medium.

Theorem 6. *Under the assumptions of Theorem 5, the solution of Step 3 of the multilevel decoupled scheme ($(J+1)-$ level method), with $j \ge 1$ is stable*

$$\kappa||\phi_{h_j}||^2_{\mathrm{DG}} \le \mathcal{D}_j^2, \tag{5.47a}$$

$$2\nu||\boldsymbol{D}(\boldsymbol{U}_{h_j})||^2_{L^2(\Omega_1)} \le \mathcal{N}_j^2, \tag{5.47b}$$

where

$$\begin{aligned}
\mathcal{D}_j &= \left[\frac{3}{\kappa}\left(\mathcal{P}_2^2||f_2||^2_{L^2(\Omega_2)}+(C_0C_1C_2)^2\frac{(\mathcal{N}_j^*)^2}{2\nu}+C_3^2||g_{\mathrm{N}}||^2_{L^2(\Gamma_{2\mathrm{N}})}\right)\right]^{\frac12}, \\
\mathcal{N}_j &= \left[\frac{3}{\nu}\left((\mathcal{P}_1C_1)^2||\boldsymbol{f}_1||^2_{L^2(\Omega_1)}+\left\{C_4\frac{\mathcal{N}_j^*}{\sqrt{2\nu}}\left(\frac{\mathcal{N}_{j-1}}{\sqrt{2\nu}}+||\boldsymbol{D}(\boldsymbol{U}_{h_{j-1}}-\boldsymbol{U}^*_{h_j})||_{L^2(\Omega_1)}\right)\right\}^2+(C_0C_1C_2)^2\frac{(\mathcal{D}_j)^2}{\kappa}\right)\right]^{\frac12}.
\end{aligned}$$

Further, if the condition $h_j = h_{j-1}^2$ holds then there exists a constant C independent of h_j such that

$$||\phi-\phi_{h_j}||_{\mathrm{DG}} \le C(h_{j-1}^3+h_j) \le Ch_j, \tag{5.48a}$$

$$||\boldsymbol{D}(\boldsymbol{u}-\boldsymbol{U}_{h_j})||_{L^2(\Omega_1)}+||p-P_{h_j}||_{L^2(\Omega_1)} \le C(h_{j-1}^3+h_j) \le Ch_j. \tag{5.48b}$$

$$||\boldsymbol{u}-\boldsymbol{U}_{h_j}||_{L^2(\Omega_1)} \le C(h_{j-1}^4+h_j^2) \le Ch_j^2. \tag{5.48c}$$

Proof. The proof follows arguments similar to Theorem 5 therefore we highlight the differences. We proceed by induction assuming that Theorem 6 holds for $j = m$, for $1 \le m \le J-1$. For the Darcy pressure bound we choose $q_2 = \phi_{m+1}$ in (4.4) and use (5.1)-(5.2) to obtain

$$\kappa||\phi_{h_{m+1}}||^2_{\mathrm{DG}} \le \frac{3\mathcal{P}_2^2}{\kappa}||f_2||^2_{L^2(\Omega_2)}+\frac{3(C_0C_1C_2)^2}{\kappa}||\boldsymbol{D}(\boldsymbol{U}^*_{h_{m+1}})||^2_{L^2(\Omega_1)}+\frac{3C_3^2}{\kappa}||g_{\mathrm{N}}||^2_{L^2(\Gamma_{2\mathrm{N}})}. \tag{5.49}$$

The result (5.47a) follows from applying Theorem 5 to bound $\boldsymbol{U}^*_{h_{m+1}}$ in (5.49). Similarly, for the velocity we choose $(\boldsymbol{v}_1, q_1) = (\boldsymbol{U}_{h_{m+1}}, P_{h_{m+1}})$ in (4.5a)-(4.5b) to obtain

$$
\begin{aligned}
&a_{\rm NS}(\boldsymbol{U}_{h_{m+1}}, \boldsymbol{U}_{h_{m+1}}) + c_{\rm NS}(\boldsymbol{U}_{h_m}; \boldsymbol{U}_{h_{m+1}}, \boldsymbol{U}_{h_{m+1}}) + c_{\rm NS}(\boldsymbol{U}_{h_{m+1}}; \boldsymbol{U}_{h_m}, \boldsymbol{U}_{h_{m+1}}) + \frac{1}{G}\big(\boldsymbol{U}_{h_{m+1}} \cdot \boldsymbol{\tau}_{12}, \boldsymbol{U}_{h_{m+1}} \cdot \boldsymbol{\tau}_{12}\big)_{\Gamma_{12}} \\
&= (\boldsymbol{f}_1, \boldsymbol{U}_{h_{m+1}})_{\Omega_1} + c_{\rm NS}(\boldsymbol{U}_{h_m}; \boldsymbol{U}^*_{h_{m+1}}, \boldsymbol{U}_{h_{m+1}}) + c_{\rm NS}(\boldsymbol{U}^*_{h_{m+1}}; \boldsymbol{U}_{h_m} - \boldsymbol{U}^*_{h_{m+1}}, \boldsymbol{U}_{h_{m+1}}) - (\phi_{h_{m+1}}, \boldsymbol{U}_{h_{m+1}} \cdot \boldsymbol{n}_{12})_{\Gamma_{12}}.
\end{aligned}
\tag{5.50}
$$

Applying Lemma 1 and inequalities in (5.1)-(5.2) as in Theorem 5 to bound terms in (5.50) yields

$$
\begin{aligned}
&\left(\nu - C_4 \frac{\mathcal{N}_m}{\sqrt{2\nu}}\right) ||\boldsymbol{D}(\boldsymbol{U}_{h_{m+1}})||^2_{L^2(\Omega_1)} \le \frac{3}{4\nu}\Bigg((\mathcal{P}_1 C_1)^2 ||\boldsymbol{f}_1||^2_{L^2(\Omega_1)} \qquad (5.51)\\
+ \quad &\left[C_4 ||\boldsymbol{D}(\boldsymbol{U}^*_{h_{m+1}})||_{L^2(\Omega_1)} \left\{ ||\boldsymbol{D}(\boldsymbol{U}_{h_m})||_{L^2(\Omega_1)} + ||\boldsymbol{D}(\boldsymbol{U}_{h_m} - \boldsymbol{U}^*_{h_{m+1}})||_{L^2(\Omega_1)} \right\} \right]^2 + (C_0 C_1 C_2)^2 ||\phi_{h_{m+1}}||^2_{\rm DG} \Bigg).
\end{aligned}
$$

We obtain (5.47b) by applying the small data condition (5.22), (5.47a), Theorem 5 and the induction hypothesis ((5.21b) and (5.48b) for $j = m$).

For the error analysis we begin by taking the difference between the fully coupled scheme (3.5a)-(3.5b) and Step 3 of the multilevel method (4.4) ,(4.5a)-(4.5b) to obtain

$$
\begin{aligned}
&\forall \boldsymbol{v}_1 \in \boldsymbol{X}_1^{h_{m+1}}, \forall q_1 \in M_1^{h_{m+1}}, q_2 \in M_2^{h_{m+1}}, \\
&a_{\rm NS}\big(\boldsymbol{U}^{h_{m+1}} - \boldsymbol{U}_{h_{m+1}}, \boldsymbol{v}_1\big) + b_{\rm NS}\big(\boldsymbol{v}_1, P^{h_{m+1}} - P_{h_{m+1}}\big) + c_{\rm NS}\big(\boldsymbol{U}_{h_m}; \boldsymbol{U}^{h_{m+1}} - \boldsymbol{U}_{h_{m+1}}, \boldsymbol{v}_1\big) \\
&+ c_{\rm NS}\big(\boldsymbol{U}^{h_{m+1}} - \boldsymbol{U}_{h_{m+1}}; \boldsymbol{U}_{h_m}, \boldsymbol{v}_1\big) + a_{\rm D}(\phi^{h_{m+1}} - \phi_{h_{m+1}}, q_2) \\
&+ \frac{1}{G}\big((\boldsymbol{U}^{h_{m+1}} - \boldsymbol{U}_{h_{m+1}}) \cdot \boldsymbol{\tau}_{12}, \boldsymbol{v}_1 \cdot \boldsymbol{\tau}_{12}\big)_{\Gamma_{12}} = \big(\phi_{h_{m+1}} - \phi^{h_{m+1}}, \boldsymbol{v}_1 \cdot \boldsymbol{n}_{12}\big)_{\Gamma_{12}} \qquad (5.52a)\\
&+ \big((\boldsymbol{U}^{h_{m+1}} - \boldsymbol{U}^*_{h_{m+1}}) \cdot \boldsymbol{n}_{12}, q_2\big)_{\Gamma_{12}} - c_{\rm NS}(\boldsymbol{U}_{h_m}; \boldsymbol{U}^*_{h_{m+1}}, \boldsymbol{v}_1) + c_{\rm NS}\big(\boldsymbol{U}^*_{h_{m+1}}; \boldsymbol{U}^*_{h_{m+1}} - \boldsymbol{U}_{h_m}, \boldsymbol{v}_1\big) \\
&+ c_{\rm NS}(\boldsymbol{U}_{h_m}; \boldsymbol{U}^{h_{m+1}}, \boldsymbol{v}_1) + c_{\rm NS}(\boldsymbol{U}^{h_{m+1}}; \boldsymbol{U}_{h_m}, \boldsymbol{v}_1) - c_{\rm NS}(\boldsymbol{U}^{h_{m+1}}; \boldsymbol{U}^{h_{m+1}}, \boldsymbol{v}_1) \\
&\forall q_1 \in M_1^h, \quad b_{\rm NS}\big(\boldsymbol{U}_{h_{m+1}} - \boldsymbol{U}^{h_{m+1}}, q_1\big) = 0. \qquad (5.52b)
\end{aligned}
$$

Setting $(\boldsymbol{v}_1, q_1) = \boldsymbol{0}$ and $q_2 = \phi^{h_{m+1}} - \phi_{h_{m+1}}$ in (5.52a)-(5.52b), it follows as in Theorem 5 by using arguments similar to [9] that

$$
\begin{aligned}
||\phi^{h_{m+1}} - \phi_{h_{m+1}}||_{\rm DG} &\le C\big\{h_{m+1} ||\boldsymbol{D}(\boldsymbol{U}^{h_{m+1}} - \boldsymbol{U}^*_{h_{m+1}})||_{L^2(\Omega_1)} + ||\boldsymbol{U}^{h_{m+1}} - \boldsymbol{U}^*_{h_{m+1}}||_{L^2(\Omega_1)}\big\} \\
&\le C\big\{h_{m+1} h_m^2 + h_{m+1}^2 + h_m^3\big\} \le C h_m^3
\end{aligned}
\tag{5.53}
$$

after applying Theorem 5, Lemma 3 and dropping high order terms.

For the velocity error, we first note that the nonlinear terms in the right hand-side of (5.52a) can be written as

$$
\begin{aligned}
&c_{\rm NS}\big(\boldsymbol{U}^*_{h_{m+1}}; \boldsymbol{U}^*_{h_{m+1}} - \boldsymbol{U}_{h_m}, \boldsymbol{v}_1\big) - c_{\rm NS}(\boldsymbol{U}_{h_m}; \boldsymbol{U}^*_{h_{m+1}}, \boldsymbol{v}_1) + c_{\rm NS}(\boldsymbol{U}_{h_m}; \boldsymbol{U}^{h_{m+1}}, \boldsymbol{v}_1) + c_{\rm NS}(\boldsymbol{U}^{h_{m+1}}; \boldsymbol{U}_{h_m}, \boldsymbol{v}_1) \\
&- c_{\rm NS}(\boldsymbol{U}^{h_{m+1}}; \boldsymbol{U}^{h_{m+1}}, \boldsymbol{v}_1) = c_{\rm NS}(\boldsymbol{U}^*_{h_{m+1}} - \boldsymbol{U}^{h_{m+1}}; \boldsymbol{U}^*_{h_{m+1}} - \boldsymbol{U}^{h_{m+1}}, \boldsymbol{v}_1) \qquad (5.54)\\
&+ c_{\rm NS}(\boldsymbol{U}^{h_{m+1}} - \boldsymbol{U}_{h_m}; \boldsymbol{U}^*_{h_{m+1}} - \boldsymbol{U}^{h_{m+1}}; \boldsymbol{v}_1) + c_{\rm NS}(\boldsymbol{U}^{h_{m+1}} - \boldsymbol{U}^*_{h_{m+1}}; \boldsymbol{U}_{h_m} - \boldsymbol{U}^{h_{m+1}}, \boldsymbol{v}_1),
\end{aligned}
$$

then by choosing $\boldsymbol{v}_1 = \boldsymbol{U}^{h_{m+1}} - \boldsymbol{U}_{h_{m+1}}$, $q_1 = P^{h_{m+1}} - P_{h_{m+1}}$ and $q_2 = 0$ in (5.52a)-(5.52b) we obtain

$$
2\nu ||\boldsymbol{D}(\boldsymbol{U}^{h_{m+1}} - \boldsymbol{U}_{h_{m+1}})||^2_{L^2(\Omega_1)} \le |N_1| + |N_\Gamma| + |N_2| + |N_3|,
\tag{5.55}
$$

where

$$
\begin{aligned}
N_1 &= -\big[c_{\mathrm{NS}}\big(\boldsymbol{U}_{h_m};\boldsymbol{U}^{h_{m+1}}-\boldsymbol{U}_{h_{m+1}},\boldsymbol{U}^{h_{m+1}}-\boldsymbol{U}_{h_{m+1}}\big)+c_{\mathrm{NS}}\big(\boldsymbol{U}^{h_{m+1}}-\boldsymbol{U}_{h_{m+1}};\boldsymbol{U}_{h_m},\boldsymbol{U}^{h_{m+1}}-\boldsymbol{U}_{h_{m+1}}\big)\big],\\
N_2 &= c_{\mathrm{NS}}(\boldsymbol{U}^*_{h_{m+1}}-\boldsymbol{U}^{h_{m+1}};\boldsymbol{U}^*_{h_{m+1}}-\boldsymbol{U}^{h_{m+1}},\boldsymbol{U}^{h_{m+1}}-\boldsymbol{U}_{h_{m+1}}),\\
N_3 &= c_{\mathrm{NS}}(\boldsymbol{U}^{h_{m+1}}-\boldsymbol{U}_{h_m};\boldsymbol{U}^*_{h_{m+1}}-\boldsymbol{U}^{h_{m+1}};\boldsymbol{U}^{h_{m+1}}-\boldsymbol{U}_{h_{m+1}})\\
&+ c_{\mathrm{NS}}(\boldsymbol{U}^{h_{m+1}}-\boldsymbol{U}^*_{h_{m+1}};\boldsymbol{U}_{h_m}-\boldsymbol{U}^{h_{m+1}},\boldsymbol{U}^{h_{m+1}}-\boldsymbol{U}_{h_{m+1}})\\
N_\Gamma &= \big(\phi_{h_{m+1}}-\phi^{h_{m+1}},(\boldsymbol{U}^{h_{m+1}}-\boldsymbol{U}_{h_{m+1}})\cdot\boldsymbol{n}_{12}\big)_{\Gamma_{12}}.
\end{aligned}
$$

We bound the above terms as in Theorem 5, using the induction assumption (5.21b) (for $j=m$), Lemma 1 and inequalities in (5.1)-(5.2) as follows

$$|N_1|\le C_4\frac{\mathcal{N}_m}{\sqrt{2\nu}}||\boldsymbol{D}(\boldsymbol{U}^{h_{m+1}}-\boldsymbol{U}_{h_{m+1}})||^2_{L^2(\Omega_1)}, \tag{5.56a}$$

$$|N_2|\le\frac{3C_4^2}{4\nu}\left\{||D(\boldsymbol{U}^*_{h_{m+1}}-\boldsymbol{U}^{h_{m+1}})||_{L^2\Omega_1}\right\}^4+\frac{\nu}{3}||\boldsymbol{D}(\boldsymbol{U}^{h_{m+1}}-\boldsymbol{U}_{h_{m+1}})||^2_{L^2(\Omega_1)} \tag{5.56b}$$

$$|N_3|\le\frac{3C_4^2}{4\nu}\left\{||\boldsymbol{D}(\boldsymbol{U}^{h_{m+1}}-\boldsymbol{U}_{h_m})||_{L^2(\Omega_1)}||\boldsymbol{D}(\boldsymbol{U}^*_{h_{m+1}}-\boldsymbol{U}^{h_{m+1}})||_{L^2(\Omega_1)}\right\}^2+\frac{\nu}{3}||\boldsymbol{D}(\boldsymbol{U}^{h_{m+1}}-\boldsymbol{U}_{h_{m+1}})||^2_{L^2(\Omega_1)} \tag{5.56c}$$

$$|N_\Gamma|\le\frac{3(C_0C_1C_2)^2}{4\nu}||\phi_{h_{m+1}}-\phi^{h_{m+1}}||^2_{\mathrm{DG}}+\frac{\nu}{3}||\boldsymbol{D}(\boldsymbol{U}^{h_{m+1}}-\boldsymbol{U}_{h_{m+1}})||^2_{L^2(\Omega_1)}. \tag{5.56d}$$

We combine the bounds (5.56a)-(5.56d) and applying the small data condition (5.22) in (5.55) to obtain

$$
\begin{gathered}
||\boldsymbol{D}(\boldsymbol{U}^{h_{m+1}}-\boldsymbol{U}_{h_{m+1}})||^2_{L^2(\Omega_1)}\le\frac{3C_4^2}{4\nu^2}\Big[\big\{||D(\boldsymbol{U}^*_{h_{m+1}}-\boldsymbol{U}^{h_{m+1}})||_{L^2\Omega_1}\big\}^4\\
+\big\{||\boldsymbol{D}(\boldsymbol{U}^{h_{m+1}}-\boldsymbol{U}_{h_m})||_{L^2(\Omega_1)}||\boldsymbol{D}(\boldsymbol{U}^*_{h_{m+1}}-\boldsymbol{U}^{h_{m+1}})||_{L^2(\Omega_1)}\big\}^2\Big]+\frac{3(C_0C_1C_2)^2}{4\nu^2}||\phi_{h_{m+1}}-\phi^{h_{m+1}}||^2_{\mathrm{DG}}
\end{gathered} \tag{5.57}
$$

Applying the triangle inequality, Lemma 3, Theorem 5, the induction hypothesis ((5.48b)-(5.48c) for $j=m$) and (5.53) to the error terms in (5.57) and dropping high order terms we can conclude that

$$||\boldsymbol{D}(\boldsymbol{U}^{h_{m+1}}-\boldsymbol{U}_{h_{m+1}})||^2_{L^2(\Omega_1)}\le C\big\{h^4_{m+1}+[(h_{m+1}+h_m)(h_m^2+h_{m+1})]^2+(h_m^3)^2\big\}\le C(h_m^3)^2 \tag{5.58}$$

For the pressure error setting $q_2=0$ in (5.52a) and using (5.54) to rewrite the nonlinear terms, it follows from the inf-sup condition (3.1) that

$$
\begin{aligned}
||P^{h_{m+1}}-P_{h_{m+1}}||_{L^2(\Omega_1)} &\le \frac{b_{\mathrm{NS}}(\boldsymbol{v}_1,P^{h_{m+1}}-P_{h_{m+1}})}{||\boldsymbol{D}(\boldsymbol{v}_1)||_{L^2(\Omega_1)}} && (5.59a)\\
&\le \frac{|a_{\mathrm{NS}}(\boldsymbol{U}^{h_{m+1}}-\boldsymbol{U}_{h_{m+1}},\boldsymbol{v}_1)|+|T_1|+|T_\Gamma|+|T_2|+|T_3|}{||\boldsymbol{D}(\boldsymbol{v}_1)||_{L^2(\Omega_1)}} && (5.59b)
\end{aligned}
$$

where the following bounds are established as in Theorem 5

$$
\begin{aligned}
|T_1| &= \big|c_{\rm NS}\big(\boldsymbol{U}_{h_m};\boldsymbol{U}^{h_{m+1}}-\boldsymbol{U}_{h_{m+1}},\boldsymbol{v}_1\big)+c_{\rm NS}\big(\boldsymbol{U}^{h_{m+1}}-\boldsymbol{U}_{h_{m+1}};\boldsymbol{U}_{h_m},\boldsymbol{v}_1\big)\big| \\
&\le C_4\frac{\mathcal{N}_m}{\sqrt{2\nu}}||\boldsymbol{D}(\boldsymbol{U}^{h_{m+1}}-\boldsymbol{U}_{h_{m+1}})||_{L^2(\Omega_1)}||\boldsymbol{D}(\boldsymbol{v}_1)||_{L^2(\Omega_1)}, \qquad (5.60a)\\
|T_\Gamma| &= \big|\big(\phi_{h_{m+1}}-\phi^{h_{m+1}},\boldsymbol{v}_1\cdot\boldsymbol{n}_{12}\big)_{\Gamma_{12}}-\frac{1}{G}\big((\boldsymbol{U}^{h_{m+1}}-\boldsymbol{U}_{h_{m+1}})\cdot\boldsymbol{\tau}_{12},\boldsymbol{v}_1\cdot\boldsymbol{\tau}_{12}\big)_{\Gamma_{12}}\big| \\
&\le C_0C_1\bigg(C_2||\phi_{h_{m+1}}-\phi^{h_{m+1}}||_{\rm DG}+\frac{1}{G}||\boldsymbol{D}(\boldsymbol{U}^{h_{m+1}}-\boldsymbol{U}_{h_{m+1}})||_{L^2(\Omega_1)}\bigg)||\boldsymbol{D}(\boldsymbol{v}_1)||_{L^2(\Omega_1)}, \qquad (5.60b)\\
|T_2| &= \big|c_{\rm NS}(\boldsymbol{U}^*_{h_{m+1}}-\boldsymbol{U}^{h_{m+1}};\boldsymbol{U}^*_{h_{m+1}}-\boldsymbol{U}^{h_{m+1}},\boldsymbol{v}_1)\big| \\
&\le C_4||\boldsymbol{D}(\boldsymbol{U}^*_{h_{m+1}}-\boldsymbol{U}^{h_{m+1}})||^2_{L^2(\Omega_1)}||\boldsymbol{D}(\boldsymbol{v}_1)||_{L^2(\Omega_1)}, \qquad (5.60c)\\
|T_3| &= \big|c_{\rm NS}(\boldsymbol{U}^{h_{m+1}}-\boldsymbol{U}_{h_m};\boldsymbol{U}^*_{h_{m+1}}-\boldsymbol{U}^{h_{m+1}};\boldsymbol{v}_1)+c_{\rm NS}(\boldsymbol{U}^{h_{m+1}}-\boldsymbol{U}^*_{h_{m+1}};\boldsymbol{U}_{h_m}-\boldsymbol{U}^{h_{m+1}},\boldsymbol{v}_1)\big| \\
&\le C_4||\boldsymbol{D}(\boldsymbol{U}^{h_{m+1}}-\boldsymbol{U}_{h_m})||_{L^2(\Omega_1)}||\boldsymbol{D}(\boldsymbol{U}^*_{h_{m+1}}-\boldsymbol{U}^{h_{m+1}})||_{L^2(\Omega_1)}||\boldsymbol{D}(\boldsymbol{v}_1)||_{L^2(\Omega_1)}. \qquad (5.60d)
\end{aligned}
$$

Combining the bounds (5.60a)-(5.60d) in (5.59b) yields

$$
\begin{aligned}
||P^{h_{m+1}}-P_{h_{m+1}}||_{L^2(\Omega_1)} &\le \bigg(2\nu+C_4\frac{\mathcal{N}_m}{\sqrt{2\nu}}+\frac{C_0C_1}{G}\bigg)||\boldsymbol{D}(\boldsymbol{U}^{h_{m+1}}-\boldsymbol{U}_{h_{m+1}})||_{L^2(\Omega_1)}+C_0C_1C_2||\phi_{h_{m+1}}-\phi^{h_{m+1}}||_{\rm DG}\\
&+ C_4\Big\{||\boldsymbol{D}(\boldsymbol{U}^*_{h_{m+1}}-\boldsymbol{U}^{h_{m+1}})||^2_{L^2(\Omega_1)}\\
&+ ||\boldsymbol{D}(\boldsymbol{U}^{h_{m+1}}-\boldsymbol{U}_{h_m})||_{L^2(\Omega_1)}||\boldsymbol{D}(\boldsymbol{U}^*_{h_{m+1}}-\boldsymbol{U}^{h_{m+1}})||_{L^2(\Omega_1)}\Big\}\\
&\le C\{h_m^3+h_m^4+h_m^2(h_{m+1}+h_m)\}\\
&\le Ch_m^3 \qquad (5.61)
\end{aligned}
$$

after applying Lemma 3, (5.34), (5.53), (5.58) and the induction hypothesis ((5.48b) for $j=m$) and dropping high order terms. Thus (5.48a)-(5.48b) follow from Lemma 3 and (5.53), (5.58) and (5.61).

Finally we prove the L_2 error bound for the Navier-Stokes velocity. We consider the following adjoint problem similar to (5.39) in Theorem 5.

$$
\begin{aligned}
&\text{Find } (\boldsymbol{w},r)\in(\boldsymbol{X}_1,M_1) \text{ s.t. } \forall\boldsymbol{v}_1\in\boldsymbol{X}_1,\forall q_1\in M_1,\\
&a_{\rm NS}(\boldsymbol{v}_1,\boldsymbol{w}_1)+b_{\rm NS}(\boldsymbol{v}_1,r)+b_{\rm NS}(\boldsymbol{w},q_1)+c_{\rm NS}(\boldsymbol{u};\boldsymbol{v}_1,\boldsymbol{w})+c_{\rm NS}(\boldsymbol{v}_1;\boldsymbol{u},\boldsymbol{w}) \qquad (5.62)\\
&+\frac{1}{G}\big(\boldsymbol{v}_1\cdot\boldsymbol{\tau}_{12},\boldsymbol{w}\cdot\boldsymbol{\tau}_{12}\big)_{\Gamma_{12}}+(\phi-\phi_{h_{m+1}},\boldsymbol{w}\cdot\boldsymbol{n}_{12})_{\Gamma_{12}}=(\boldsymbol{g}_1,\boldsymbol{v}_1)_{\Omega_1}.
\end{aligned}
$$

where $(\boldsymbol{u},\phi)$ is a nonsingular solution of (2.4a)-(2.4b) satisfying the H^2-regularity assumption

$$
||\boldsymbol{w}||_{H^2(\Omega_1)}+||r||_{H^1(\Omega_1)}\le C||\boldsymbol{g}_1||_{L^2(\Omega_1)}. \qquad (5.63)
$$

Setting $\boldsymbol{g}_1=\boldsymbol{u}-\boldsymbol{U}_{h_{m+1}}$ and $(\boldsymbol{v}_1,q_1)=(\boldsymbol{u}-\boldsymbol{U}_{h_{m+1}},p-P_{h_{m+1}})$ in (5.62) and splitting the nonlinear terms yields

$$
\begin{aligned}
||\boldsymbol{u}-\boldsymbol{U}_{h_{m+1}}||^2_{L^2(\Omega_1)} &= a_{\rm NS}(\boldsymbol{u}-\boldsymbol{U}_{h_{m+1}},\boldsymbol{w})+b_{\rm NS}(\boldsymbol{u}-\boldsymbol{U}_{h_{m+1}},r)+b_{\rm NS}(\boldsymbol{w},p-P_{h_{m+1}})\\
&+ c_{\rm NS}(\boldsymbol{U}_{h_m};\boldsymbol{u}-\boldsymbol{U}_{h_{m+1}},\boldsymbol{w})+c_{\rm NS}(\boldsymbol{u}-\boldsymbol{U}_{h_{m+1}};\boldsymbol{U}_{h_m},\boldsymbol{w})\\
&+ \frac{1}{G}((\boldsymbol{u}-\boldsymbol{U}_{h_{m+1}})\cdot\boldsymbol{\tau}_{12},\boldsymbol{w}\cdot\boldsymbol{\tau}_{12})_{\Gamma_{12}}+(\phi-\phi_{h_{m+1}},\boldsymbol{w}\cdot\boldsymbol{n}_{12})_{\Gamma_{12}}\\
&+ c_{\rm NS}(\boldsymbol{u}-\boldsymbol{U}_{h_m};\boldsymbol{u}-\boldsymbol{U}_{h_{m+1}},\boldsymbol{w})+c_{\rm NS}(\boldsymbol{u}-\boldsymbol{U}_{h_{m+1}};\boldsymbol{u}-\boldsymbol{U}_{h_m},\boldsymbol{w}) \qquad (5.64)
\end{aligned}
$$

Setting $q_2 = 0$ in (2.4a)-(2.4b) and subtracting Step 3 of the multilevel method (4.5a)-(4.5b) yields

$$\begin{aligned} & a_{\text{NS}}(\boldsymbol{u} - \boldsymbol{U}_{h_{m+1}}, \boldsymbol{v}_1) + b_{\text{NS}}(\boldsymbol{u} - \boldsymbol{U}_{h_{m+1}}, q_1) + b_{\text{NS}}(\boldsymbol{v}_1, p - P_{h_{m+1}}) + c_{\text{NS}}(\boldsymbol{U}_{h_m}; \boldsymbol{u} - \boldsymbol{U}_{h_{m+1}}, \boldsymbol{v}_1) \\ & + c_{\text{NS}}(\boldsymbol{u} - \boldsymbol{U}_{h_{m+1}}; \boldsymbol{U}_{h_m}, \boldsymbol{v}_1) + (\phi - \phi_{h_{m+1}}, \boldsymbol{v}_1 \cdot \boldsymbol{n}_{12})_{\Gamma_{12}} + \frac{1}{G}\big((\boldsymbol{u} - \boldsymbol{U}_{h_{m+1}}) \cdot \boldsymbol{\tau}_{12}, \boldsymbol{v}_1 \cdot \boldsymbol{\tau}_{12}\big)_{\Gamma_{12}} \\ & + c_{\text{NS}}(\boldsymbol{u} - \boldsymbol{U}_{h_m}; \boldsymbol{u} - \boldsymbol{U}^*_{h_{m+1}}, \boldsymbol{v}_1) + c_{\text{NS}}(\boldsymbol{u} - \boldsymbol{U}^*_{h_{m+1}}; \boldsymbol{u} - \boldsymbol{U}_{h_m}, \boldsymbol{v}_1) - c_{\text{NS}}(\boldsymbol{u} - \boldsymbol{U}^*_{h_{m+1}}; \boldsymbol{u} - \boldsymbol{U}^*_{h_{m+1}}, \boldsymbol{v}_1) = 0. \end{aligned} \tag{5.65}$$

Subtracting the error term (5.65) in the right hand side of (5.64), we obtain

$$\begin{aligned} ||\boldsymbol{u} - \boldsymbol{U}_{h_{m+1}}||^2_{L^2(\Omega_1)} &= a_{\text{NS}}(\boldsymbol{u} - \boldsymbol{U}_{h_{m+1}}, \boldsymbol{w} - \boldsymbol{v}_1) + b_{\text{NS}}(\boldsymbol{u} - \boldsymbol{U}_{h_{m+1}}, r - q_1) + b_{\text{NS}}(\boldsymbol{w} - \boldsymbol{v}_1, p - P_{h_{m+1}}) \\ &+ c_{\text{NS}}(\boldsymbol{U}_{h_m}; \boldsymbol{u} - \boldsymbol{U}_{h_{m+1}}, \boldsymbol{w} - \boldsymbol{v}_1) + c_{\text{NS}}(\boldsymbol{u} - \boldsymbol{U}_{h_{m+1}}; \boldsymbol{U}_{h_m}, \boldsymbol{w} - \boldsymbol{v}_1) \\ &+ (\phi - \phi_{h_{m+1}}, (\boldsymbol{w} - \boldsymbol{v}_1) \cdot \boldsymbol{n}_{12})_{\Gamma_{12}} + \frac{1}{G}\big((\boldsymbol{u} - \boldsymbol{U}_{h_{m+1}}) \cdot \boldsymbol{\tau}_{12}, (\boldsymbol{w} - \boldsymbol{v}_1) \cdot \boldsymbol{\tau}_{12}\big)_{\Gamma_{12}} \\ &+ c_{\text{NS}}(\boldsymbol{u} - \boldsymbol{U}_{h_m}; \boldsymbol{u} - \boldsymbol{U}_{h_{m+1}}, \boldsymbol{w}) + c_{\text{NS}}(\boldsymbol{u} - \boldsymbol{U}_{h_{m+1}}; \boldsymbol{u} - \boldsymbol{U}_{h_m}, \boldsymbol{w}) \\ &- c_{\text{NS}}(\boldsymbol{u} - \boldsymbol{U}_{h_m}; \boldsymbol{u} - \boldsymbol{U}^*_{h_{m+1}}, \boldsymbol{v}_1) - c_{\text{NS}}(\boldsymbol{u} - \boldsymbol{U}^*_{h_{m+1}}; \boldsymbol{u} - \boldsymbol{U}_{h_m}, \boldsymbol{v}_1) \\ &+ c_{\text{NS}}(\boldsymbol{u} - \boldsymbol{U}^*_{h_{m+1}}; \boldsymbol{u} - \boldsymbol{U}^*_{h_{m+1}}, \boldsymbol{v}_1) = 0. \end{aligned} \tag{5.66}$$

We bound the terms in (5.66) in a manner similar to (5.44a)-(5.44c) in Theorem 5 as follows

$$\big|a_{\text{NS}}(\boldsymbol{u} - \boldsymbol{U}_{h_{m+1}}, \boldsymbol{w} - \boldsymbol{v}_1)\big| \leq Ch^2_{m+1}||\boldsymbol{g}_1||_{L^2(\Omega_1)}, \tag{5.67a}$$

$$\big|b_{\text{NS}}(\boldsymbol{u} - \boldsymbol{U}_{h_{m+1}}, r - q_1) + b_{\text{NS}}(\boldsymbol{w} - \boldsymbol{v}_1, p - P_{h_{m+1}})\big| \leq Ch^2_{m+1}||\boldsymbol{g}_1||_{L^2(\Omega_1)}. \tag{5.67b}$$

Similarly as in (5.45) we obtain

$$\begin{aligned} \big|(\phi - \phi_{h_{m+1}}, (\boldsymbol{w} - \boldsymbol{v}_1) \cdot \boldsymbol{n}_{12})_{\Gamma_{12}} &+ \frac{1}{G}\big((\boldsymbol{u} - \boldsymbol{U}_{h_{m+1}}) \cdot \boldsymbol{\tau}_{12}, (\boldsymbol{w} - \boldsymbol{v}_1) \cdot \boldsymbol{\tau}_{12}\big)_{\Gamma_{12}}\big| \\ &\leq Ch^2_{m+1}||\boldsymbol{g}_1||_{L^2(\Omega_1)}. \end{aligned} \tag{5.68}$$

Using Lemma 1, Theorem 5, (5.63) and the induction hypothesis ((5.21b) and (5.48b)-(5.48c) for $j = m$) the following bounds hold

$$\begin{aligned} \big|c_{\text{NS}}(\boldsymbol{U}_{h_m}; \boldsymbol{u} - \boldsymbol{U}_{h_{m+1}}, \boldsymbol{w} - \boldsymbol{v}_1) &+ c_{\text{NS}}(\boldsymbol{u} - \boldsymbol{U}_{h_{m+1}}; \boldsymbol{U}_{h_m}, \boldsymbol{w} - \boldsymbol{v}_1)\big| \\ &\leq C_4||\boldsymbol{D}(\boldsymbol{U}_{h_m})||_{L^2(\Omega_1)}||\boldsymbol{D}(\boldsymbol{u} - \boldsymbol{U}_{h_{m+1}})||_{L^2(\Omega_1)}||\boldsymbol{D}(\boldsymbol{w} - \boldsymbol{v}_1)||_{L^2(\Omega_1)} \\ &\leq C(h^2_m + h_{m+1})h_{m+1}||\boldsymbol{g}_1||_{L^2(\Omega_1)} && (5.69\text{a}) \\ \big|c_{\text{NS}}(\boldsymbol{u} - \boldsymbol{U}_{h_m}; \boldsymbol{u} - \boldsymbol{U}_{h_{m+1}}, \boldsymbol{w}) &+ c_{\text{NS}}(\boldsymbol{u} - \boldsymbol{U}_{h_{m+1}}; \boldsymbol{u} - \boldsymbol{U}_{h_m}, \boldsymbol{w})\big| \\ &\leq C_4||\boldsymbol{u} - \boldsymbol{U}_{h_m}||_{L^2(\Omega_1)}||\boldsymbol{D}(\boldsymbol{u} - \boldsymbol{U}_{h_{m+1}})||_{L^2(\Omega_1)}||\boldsymbol{w}||_{H^2(\Omega_1)} \\ &\leq Ch^2_m(h^2_m + h_{m+1})||\boldsymbol{g}_1||_{L^2(\Omega_1)} && (5.69\text{b}) \\ \big|c_{\text{NS}}(\boldsymbol{u} - \boldsymbol{U}_{h_m}; \boldsymbol{u} - \boldsymbol{U}^*_{h_{m+1}}, \boldsymbol{v}_1)\big| &\leq \big|c_{\text{NS}}(\boldsymbol{u} - \boldsymbol{U}_{h_m}; \boldsymbol{u} - \boldsymbol{U}^*_{h_{m+1}}, \boldsymbol{w} - \boldsymbol{v}_1)\big| + \big|c_{\text{NS}}(\boldsymbol{u} - \boldsymbol{U}_{h_m}; \boldsymbol{u} - \boldsymbol{U}^*_{h_{m+1}}, \boldsymbol{w})\big| \\ &\leq C_4\big\{||\boldsymbol{D}(\boldsymbol{u} - \boldsymbol{U}_{h_m})||_{L^2(\Omega_1)}||\boldsymbol{D}(\boldsymbol{u} - \boldsymbol{U}^*_{h_{m+1}})||_{L^2(\Omega_1)}||\boldsymbol{D}(\boldsymbol{w} - \boldsymbol{v}_1)||_{L^2(\Omega_1)} \\ &+ ||\boldsymbol{u} - \boldsymbol{U}_{h_m}||_{L^2(\Omega_1)}||\boldsymbol{D}(\boldsymbol{u} - \boldsymbol{U}^*_{h_{m+1}})||_{L^2(\Omega_1)}||\boldsymbol{w}||_{H^2(\Omega_1)}\big\} \\ &\leq C\big\{h_m(h^2_m + h_{m+1})h_{m+1} + h^2_m(h^2_m + h_{m+1})\big\}||\boldsymbol{g}_1||_{L^2(\Omega_1)} && (5.69\text{c}) \end{aligned}$$

$$
\begin{aligned}
\left|c_{\mathrm{NS}}(\boldsymbol{u}-\boldsymbol{U}^*_{h_{m+1}};\boldsymbol{u}-\boldsymbol{U}_{h_m},\boldsymbol{v}_1)\right| &\le \left|c_{\mathrm{NS}}(\boldsymbol{u}-\boldsymbol{U}^*_{h_{m+1}};\boldsymbol{u}-\boldsymbol{U}_{h_m},\boldsymbol{w}-\boldsymbol{v}_1)\right| + \left|c_{\mathrm{NS}}(\boldsymbol{u}-\boldsymbol{U}^*_{h_{m+1}};\boldsymbol{u}-\boldsymbol{U}_{h_m},\boldsymbol{w})\right| \\
&\le C_4\big\{||\boldsymbol{D}(\boldsymbol{u}-\boldsymbol{U}^*_{h_{m+1}})||_{L^2(\Omega_1)}||\boldsymbol{D}(\boldsymbol{u}-\boldsymbol{U}_{h_m})||_{L^2(\Omega_1)}||\boldsymbol{D}(\boldsymbol{w}-\boldsymbol{v}_1)||_{L^2(\Omega_1)} \\
&+ ||\boldsymbol{D}(\boldsymbol{u}-\boldsymbol{U}^*_{h_{m+1}})||_{L^2(\Omega_1)}||\boldsymbol{u}-\boldsymbol{U}_{h_m}||_{L^2(\Omega_1)}||\boldsymbol{w}||_{H^2(\Omega_1)}\big\} \\
&\le C\big\{(h_m^2+h_{m+1})h_m h_{m+1} + (h_m^2+h_{m+1})h_m^2\big\}||\boldsymbol{g}_1||_{L^2(\Omega_1)} \qquad (5.70a) \\
\left|c_{\mathrm{NS}}(\boldsymbol{u}-\boldsymbol{U}^*_{h_{m+1}};\boldsymbol{u}-\boldsymbol{U}^*_{h_{m+1}},\boldsymbol{v}_1)\right| &\le \left|c_{\mathrm{NS}}(\boldsymbol{u}-\boldsymbol{U}^*_{h_{m+1}};\boldsymbol{u}-\boldsymbol{U}^*_{h_{m+1}},\boldsymbol{w}-\boldsymbol{v}_1)\right| + \left|c_{\mathrm{NS}}(\boldsymbol{u}-\boldsymbol{U}^*_{h_{m+1}};\boldsymbol{u}-\boldsymbol{U}^*_{h_{m+1}},\boldsymbol{v}_1)\right| \\
&\le C_4\big\{||\boldsymbol{D}(\boldsymbol{u}-\boldsymbol{U}^*_{h_{m+1}})||^2_{L^2(\Omega_1)}||\boldsymbol{D}(\boldsymbol{w}-\boldsymbol{v}_1)||_{L^2(\Omega_1)} \\
&+ ||\boldsymbol{D}(\boldsymbol{u}-\boldsymbol{U}^*_{h_{m+1}})||_{L^2(\Omega_1)}||\boldsymbol{u}-\boldsymbol{U}^*_{h_{m+1}}||_{L^2(\Omega_1)}||\boldsymbol{w}||_{H^2(\Omega_1)}\big\} \\
&\le C\{(h_m^2+h_{m+1})h_{m+1} + (h_m^2+h_{m+1})(h_m^3+h_{m+1}^2)\}||\boldsymbol{g}_1||_{L^2(\Omega_1)} \qquad (5.70b)
\end{aligned}
$$

We conclude by combining (5.67a)-(5.70b) to obtain

$$||\boldsymbol{u}-\boldsymbol{U}_{h_{m+1}}||_{L^2(\Omega_1)} \le C(h_m^4 + h_{m+1}^2).$$

after dropping high order terms assuming the mesh relation $h_{m+1} = h_m^2$.

6. Numerical results

In this section we present numerical results to verify the convergence of the multilevel method and compare its accuracy and efficiency relative to the fully coupled one-level method. For the comparative study both the fully coupled and multilevel methods are implemented on the same computational platform and all linear systems are are solved by the solver MUMPS [2, 3]. For the convergence study we consider a first order numerical scheme with the Navier–Stokes velocity and pressure are approximated by the first order MINI element and the Darcy pressure is approximated by the NIPG method (i.e. $\epsilon = 1$ and $\sigma = 1$ in (3.4)) using linear discontinuous polynomials.

6.1. Convergence of multilevel method

We begin with a test problem with a known smooth solution to verify theoretical convergence rates of the multilevel scheme. The boundary conditions and source functions are chosen so that the exact solution to the coupled Navier–Stokes/Darcy problem is

$$
\begin{aligned}
\boldsymbol{u}(x,y) &= \big(-\cos(\pi x)\sin(\pi y), \sin(\pi x)\cos(\pi y)\big), \\
p(x,y) &= \frac{y^2}{2}\sin(\pi x), \phi(x,y) = \frac{y^2}{2}\sin(\pi x).
\end{aligned}
$$

The computational domain $\Omega = [0,1]\times[0,2]$ is subdivided into $\Omega_1 = [0,1]\times[1,2]$ and $\Omega_2 = [0,1]\times[0,1]$ with the interface Γ_{12} along $y = 1$. We prescribe Dirichlet boundary conditions on the free flow boundary Γ_1. On Γ_2, we prescribe Dirichlet and Neumann boundary conditions on the horizontal and lateral boundary edges, respectively. The physical parameters ν, G and k are set to 1.0. For comparison, we first show the convergence of the fully coupled scheme in Table 1. The observed convergence is optimal; first order in the

$1/h$	$\|\|p-P^h\|\|_0$	$\|\|\boldsymbol{D}(\boldsymbol{u}-\boldsymbol{U}^h)\|\|_0$	$\|\|\phi-\phi^h\|\|_{\mathrm{DG}}$	$\|\|\phi-\phi^h\|\|_0$	$\|\|\boldsymbol{u}-\boldsymbol{U}^h\|\|_0$
2	2.447×10^{1}	4.290×10^{0}	5.461×10^{-1}	9.499×10^{-2}	2.088×10^{-1}
4	1.927×10^{0}	1.131×10^{0}	2.826×10^{-1}	2.423×10^{-2}	9.426×10^{-2}
16	1.505×10^{-1}	2.633×10^{-1}	7.139×10^{-2}	1.529×10^{-3}	5.747×10^{-3}
256	2.146×10^{-3}	1.632×10^{-2}	4.509×10^{-3}	5.980×10^{-6}	2.267×10^{-5}
rate	1.53	1.00	1.00	2.00	2.00

Table 1: Errors and convergence of fully coupled scheme

energy and DG norms for the Navier–Stokes velocity and Darcy pressure errors, respectively and second order in the L_2-norm for the velocity and Darcy pressure. The fluid pressure error converges at a rate better than first order, this is consistent with other implementations of the MINI element in the literature.

To determine the convergence of the multilevel method we start with the same coarse mesh of size h_0 and compare the solution on successively finer meshes h_j satisfying $h_j = h_{j-1}^2$ for $j \geq 1$. For example, in Table 2 the solution from a mesh of size $h = \frac{1}{4}$ is obtained from a two-level method with the fully coupled problem solved on a mesh with $h_0 = \frac{1}{2}$ and decoupled problems on $h = \frac{1}{4}$. Similarly, the solution on a mesh with $h = \frac{1}{16}$ is generated by a three-level method starting with $h_0 = \frac{1}{2}$ and decoupled problems solved on $h_1 = \frac{1}{4}$ and $h_2 = \frac{1}{16}$. In Table 2 we observe the expected first order convergence in the energy norm and

Mesh levels	$\|\|p - P_{h_j}\|\|_0$	$\|\|\boldsymbol{D}(\boldsymbol{u} - \boldsymbol{U}_{h_j})\|\|_0$	$\|\|\phi - \phi_{h_j}\|\|_{\mathrm{DG}}$	$\|\|\phi - \phi_{h_j}\|\|_0$	$\|\|\boldsymbol{u} - \boldsymbol{U}_{h_j}\|\|_0$
$\frac{1}{2}, \frac{1}{4}$	2.812×10^{0}	1.351×10^{0}	2.844×10^{-1}	2.337×10^{-2}	6.965×10^{-2}
$\frac{1}{2}, \frac{1}{4}, \frac{1}{16}$	2.586×10^{-1}	3.086×10^{-1}	7.467×10^{-2}	1.432×10^{-3}	4.482×10^{-3}
$\frac{1}{2}, \frac{1}{4}, \frac{1}{16}, \frac{1}{256}$	3.551×10^{-3}	1.886×10^{-2}	4.735×10^{-3}	5.628×10^{-6}	1.781×10^{-5}
rate	1.54	1.00	1.00	2.00	2.00

Table 2: Errors and convergence of multilevel method with $h_0 = \frac{1}{2}$, $h_j = h_{j-1}^2$

second order in the L_2 norm for the Navier–Stokes velocity. The convergence of the Darcy pressure in the L_2 norm also appears to be optimal though we have no formal proof of this result. To study the effect of the size of the initial coarse mesh, we repeat the convergence study with a finer initial coarse mesh with $h_0 = \frac{1}{4}$.

Mesh levels	$\|\|p - P_{h_j}\|\|_0$	$\|\|\boldsymbol{D}(\boldsymbol{u} - \boldsymbol{U}_{h_j})\|\|_0$	$\|\|\phi - \phi_{h_j}\|\|_{\mathrm{DG}}$	$\|\|\phi - \phi_{h_j}\|\|_0$	$\|\|\boldsymbol{u} - \boldsymbol{U}_{h_j}\|\|_0$
$\frac{1}{4}, \frac{1}{16}$	1.883×10^{-1}	2.754×10^{-1}	7.274×10^{-2}	1.481×10^{-3}	6.033×10^{-3}
$\frac{1}{4}, \frac{1}{16}, \frac{1}{256}$	2.804×10^{-3}	1.699×10^{-2}	4.599×10^{-3}	7.048×10^{-6}	2.330×10^{-5}
rate	1.52	1.00	1.00	1.93	2.00

Table 3: Errors and convergence of multilevel method with $h_0 = \frac{1}{4}$, $h_j = h_{j-1}^2$

Table 3 shows the errors and convergence rates for the multilevel method with $h_0 = \frac{1}{4}$. The observed convergence rates are optimal and we note that the order of magnitude of the errors for the decoupling scheme with initial coarse meshes with $h_0 = \frac{1}{4}$ and $h_0 = \frac{1}{2}$ are the same; showing that even with a very coarse initial mesh the multilevel method gives a good approximation to the coupled problem.

Mesh levels	$\|\|p - P_{h_j}^*\|\|_0$	$\|\|\boldsymbol{D}(\boldsymbol{u} - \boldsymbol{U}_{h_j}^*)\|\|_0$	$\|\|\phi - \phi_{h_j}^*\|\|_{\mathrm{DG}}$	$\|\|\phi - \phi_{h_j}^*\|\|_0$	$\|\|\boldsymbol{u} - \boldsymbol{U}_{h_j}^*\|\|_0$
$\frac{1}{4}, \frac{1}{16}$	1.831×10^{-1}	2.753×10^{-1}	8.888×10^{-2}	1.973×10^{-2}	5.957×10^{-3}
$\frac{1}{4}, \frac{1}{16}, \frac{1}{256}$	3.403×10^{-3}	1.699×10^{-2}	5.547×10^{-3}	1.198×10^{-3}	2.669×10^{-5}
rate	1.43	1.00	1.00	1.00	1.95

Table 4: Errors and convergence of multilevel method without correction step with $h_0 = \frac{1}{4}$, $h_j = h_{j-1}^2$

We conclude the section by discussing the need for the correction step for the multi-level method. Table 4 shows the errors and convergence rate of the intermediate solution $(\boldsymbol{U}_{h_j}^*, P_{h_j}^*, \phi_{h_j}^*)$. We observe optimal convergence in both the L_2 and H_1 norms in the free flow region. However, the L_2 norm of the pressure in the porous medium is suboptimal due to the fact that the coarse mesh velocity is used as a boundary condition for the Darcy decoupled problem. A comparison of Tables 3 and 4 shows that the correction step results in significant improvements in the pressure error in the porous media flow region. The gains in accuracy in the free flow region are modest due to the fact that the pressure solution used in the intermediate solution is from the fine mesh.

6.2. Accuracy and computational efficiency

Using the same problem set up as in the previous section, we compare the accuracy and efficiency of the multilevel method to solving the fully coupled approach. For various mesh sizes, we provide the errors and

CPU times for the solution obtained from the fully coupled (one-level method) and the solution obtained using a multilevel method where the decoupled problems are solved on a sequence of meshes up to h starting with a coarse mesh h_0. We compare the errors and CPU times; for example, in the first set of test problems

Grid levels	$\|\|p - P_{h_j}\|\|_0$	$\|\|\boldsymbol{D}(\boldsymbol{u} - \boldsymbol{U}_{h_j})\|\|_0$	$\|\|(\boldsymbol{u} - \boldsymbol{U}_{h_j})\|\|_0$	$\|\|\phi - \phi_{h_j}\|\|_{\mathrm{DG}}$	$\|\|\phi - \phi_{h_j}\|\|_0$	CPU(s)
$\frac{1}{16}$	1.504×10^{-1}	2.633×10^{-1}	5.747×10^{-3}	7.139×10^{-2}	1.529×10^{-3}	1.11
$\frac{1}{4}, \frac{1}{16}$	1.834×10^{-1}	2.754×10^{-1}	6.033×10^{-3}	7.274×10^{-2}	1.481×10^{-3}	0.45
$\frac{1}{2}, \frac{1}{4}, \frac{1}{16}$	2.586×10^{-1}	3.086×10^{-1}	4.482×10^{-3}	7.467×10^{-2}	1.432×10^{-3}	0.41
$\frac{1}{64}$	1.746×10^{-2}	6.541×10^{-2}	3.624×10^{-4}	1.780×10^{-2}	9.567×10^{-5}	16.19
$\frac{1}{8}, \frac{1}{64}$	1.850×10^{-2}	6.566×10^{-2}	3.683×10^{-4}	1.806×10^{-2}	9.287×10^{-5}	6.06
$\frac{1}{256}$	2.146×10^{-3}	1.632×10^{-2}	2.267×10^{-5}	4.509×10^{-3}	5.980×10^{-6}	309.49
$\frac{1}{16}, \frac{1}{256}$	2.164×10^{-3}	1.632×10^{-2}	2.280×10^{-5}	4.512×10^{-3}	6.802×10^{-6}	98.77
$\frac{1}{4}, \frac{1}{16}, \frac{1}{256}$	2.804×10^{-3}	1.699×10^{-2}	2.330×10^{-5}	4.599×10^{-3}	7.048×10^{-6}	98.06
$\frac{1}{2}, \frac{1}{4}, \frac{1}{16}, \frac{1}{256}$	3.551×10^{-3}	1.886×10^{-2}	1.781×10^{-5}	4.735×10^{-3}	5.628×10^{-6}	97.90

Table 5: Comparison of multilevel method with fully coupled method

in Table 5, we solve the fully coupled nonlinear problem on a mesh of size $h = \frac{1}{16}$ and compare the CPU times and accuracy to a two-level method with meshes $(\frac{1}{4}, \frac{1}{16})$ and a three-level method with meshes $(\frac{1}{2}, \frac{1}{4}, \frac{1}{16})$. In Table 5, we observe that the multilevel method is able to attain the same order of approximation as the fully coupled problem even with a very coarse initial mesh of $h = \frac{1}{2}$. For all mesh resolutions considered the multilevel method takes significantly less CPU time compared to solving the fully coupled problem (even for the three and four-level methods). Even though the majority of the computational gains are attained by the two-level method, it is clear that the multilevel method with small non-linear problem is able to attain the same order of approximation as the fully coupled problem. As we noted in Remark 1, step 2 of the

Grid levels	$\|\|p - P_{h_j}\|\|_0$	$\|\|\boldsymbol{D}(\boldsymbol{u} - \boldsymbol{U}_{h_j})\|\|_0$	$\|\|(\boldsymbol{u} - \boldsymbol{U}_{h_j})\|\|_0$	$\|\|\phi - \phi_{h_j}\|\|_{\mathrm{DG}}$	$\|\|\phi - \phi_{h_j}\|\|_0$	CPU(s)
$\frac{1}{16}$	1.504×10^{-1}	2.633×10^{-1}	5.747×10^{-3}	7.139×10^{-2}	1.529×10^{-3}	1.11
$\frac{1}{4}, \frac{1}{16}$	1.884×10^{-1}	2.754×10^{-1}	6.027×10^{-3}	7.291×10^{-2}	6.027×10^{-3}	0.45
$\frac{1}{2}, \frac{1}{4}, \frac{1}{16}$	2.586×10^{-1}	3.086×10^{-1}	4.483×10^{-3}	7.474×10^{-2}	1.459×10^{-3}	0.41
$\frac{1}{64}$	1.746×10^{-2}	6.541×10^{-2}	3.624×10^{-4}	1.780×10^{-2}	9.567×10^{-5}	16.19
$\frac{1}{8}, \frac{1}{64}$	1.853×10^{-2}	6.566×10^{-2}	3.694×10^{-4}	1.814×10^{-2}	1.476×10^{-4}	6.11
$\frac{1}{256}$	2.146×10^{-3}	1.632×10^{-2}	2.267×10^{-5}	4.509×10^{-3}	5.980×10^{-6}	309.49
$\frac{1}{16}, \frac{1}{256}$	2.174×10^{-3}	1.632×10^{-2}	2.444×10^{-5}	4.598×10^{-3}	7.114×10^{-5}	98.85
$\frac{1}{4}, \frac{1}{16}, \frac{1}{256}$	2.806×10^{-3}	1.699×10^{-2}	2.359×10^{-5}	4.618×10^{-3}	3.118×10^{-5}	97.72
$\frac{1}{2}, \frac{1}{4}, \frac{1}{16}, \frac{1}{256}$	3.554×10^{-3}	1.886×10^{-2}	1.923×10^{-5}	4.755×10^{-3}	3.371×10^{-5}	97.70

Table 6: Comparison of multilevel method (with $\phi^*_{h_{j-1}}$ on interface in Step 2(ii)) with fully coupled method

multilevel scheme in parallel. In Table 6 we list the errors from this modification of the decoupling scheme. It is clear in Table 6 that with the exception of the L_2 error for the Darcy pressure the decoupling scheme attains the same order of errors as the fully coupled scheme. However, the errors are larger than in Table 5 particularly in the case of the L_2-norm of the Darcy pressure.

In the numerical tests on smooth solutions we have presented a first order scheme i.e first order MINI elements in Ω_1 and linear DG elements in Ω_2. Due to ease of implementation we can choose higher order DG elements in Ω_2, this results in a more accurate pressure solution; however, the global convergence of the scheme remains first order due to the first order elements in Ω_1. In numerical results that follow, we use discontinuous quadratic elements to obtain a more accurate Darcy pressure solution.

6.3. Parabolic Interface

We consider a coupled flow problem in a rectangular domain with a parabolic interface; see Figure 1. We prescribe $\boldsymbol{u}_1 = (0, -1)$ on Γ_1 along $y = 2$ and a no-slip condition on the rest of the boundary. In the porous medium, we prescribe homogeneous Dirichlet boundary conditions on the horizontal boundary ($y = 0$) and

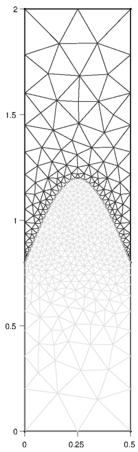

Figure 1: Parabolic interface coarse mesh: Ω_1 (black) and Ω_2 (grey)

zero Neumann boundary conditions on the lateral edges. The external forcing functions in both domains are set to zero, $\nu = 1.0$, k is varied and the parameter $G = \frac{0.1}{\sqrt{k}}$ as in [7].

We solve the problem using the multilevel method. First, a small nonlinear coupled problem of size 4974 is solved on an unstructured coarse mesh with elements of characteristic lengths of 0.025 and 0.25 near the parabolic interface and the rest of the domain, respectively; see Figure 1. The choice of this unstructured mesh enables better resolution of the parabolic interface and also allows for a numerical test with a significant number of degrees of freedom on the interface to test the robustness of the decoupling method. We apply a three-level method with meshes $(\frac{1}{4}, \frac{1}{16}, \frac{1}{64})$. The solutions plotted in Figure 2 are obtained by solving two problems of size 204105 and 1058304 in Ω_1 and Ω_2, respectively. Figure 2 is a plot of the norm of the

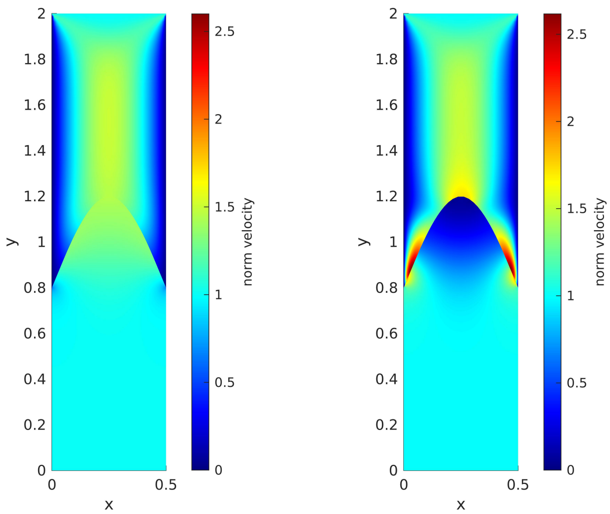

(a) $k = 1.0 \times 10^{-2}$ (b) $k = 1.0 \times 10^{-4}$

Figure 2: Norm of velocity for numerical solution on parabolic interface for $\nu = 1.0$

velocity on the finest mesh for values of $k = 1.0 \times 10^{-2}$ and 1.0×10^{-4}. We observe the expected symmetric flow pattern with a larger norm of velocity in the porous medium with a higher hydraulic conductivity in

Figure 2a compared to Figure 2b. The low hydraulic conductivity of $1.0 \times 10^{-4}\boldsymbol{I}$ in Figure 2b forces the flow around the low permeability porous medium towards the edges of the domain.

6.4. Porous medium with discontinuous hydraulic conductivity

In most practical applications the hydraulic conductivity maybe discontinuous due to heterogeneities in the porous medium. We consider a coupled flow problem with a discontinuous porous medium. The coarse mesh of the multilevel method is shown in Figure 3. The boundary conditions and data functions are set up

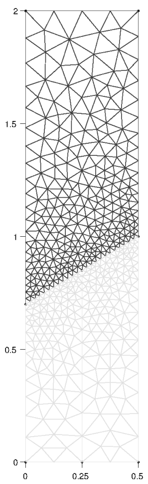

Figure 3: Slant interface with discontinuity in porous medium: Ω_1 (black) and Ω_2 (grey)

as in the previous problem. The porous medium is portioned into two regions with hydraulic conductivity $k_1\boldsymbol{I}$ and $k_2\boldsymbol{I}$ with $k_1 = 3.0 \times 10^{-4}$ and $k_2 = 1.5 \times 10^{-4}$ for $0.0 \leq x \leq 0.25$ and $0.25 \leq x \leq 0.5$, respectively. The kinematic viscosity $\nu = 1.0$ and the interface constant G is defined as in the previous example. The solutions presented are from a three-level method with a coarse mesh with elements of characteristic lengths 0.0125 and 0.125 near the interface and on the rest of the domain, respectively. The fully coupled problem on the coarse grid is of size 4534. On levels mesh levels $(\frac{1}{4}, \frac{1}{16}, \frac{1}{64})$, we solve decoupled problems in each domain. The solutions plotted are from decoupled problems of size 473329 and 683520 in Ω_1 and Ω_2, respectively. Figure 4a shows that the multilevel scheme is able to clearly resolve the sharp discontinuity in the material permeability. The fluid flow in Ω_1 is biased towards the side of the domain that has higher permeability. The relatively low permeability in the porous medium causes a build up of pressure in Ω_1 as the fluid as shown in Figure 4b. A closer look at the velocity vectors in Figure 5 near the interface reveals the expected flow pattern showing the effect of the slope on the interface and the discontinuity in the porous medium with larger velocity vectors on the left side of the computational domain in Ω_2. This problem highlights the advantage of the DG method because the numerical scheme is able to resolve the sharp discontinuity in the material permeability.

7. Conclusions

We have presented a multilevel decoupling technique for the Navier–Stokes/Darcy problem. The proposed multilevel scheme exhibits the same order of convergence as the fully coupled approach even for very coarse initial meshes. The scheme is computationally efficient and comparable in accuracy to the fully coupled problem. Numerical tests on practical test problems varying the shape of the interface and the hydraulic conductivity yield the expected flow profiles showing that the decoupling method is robust.

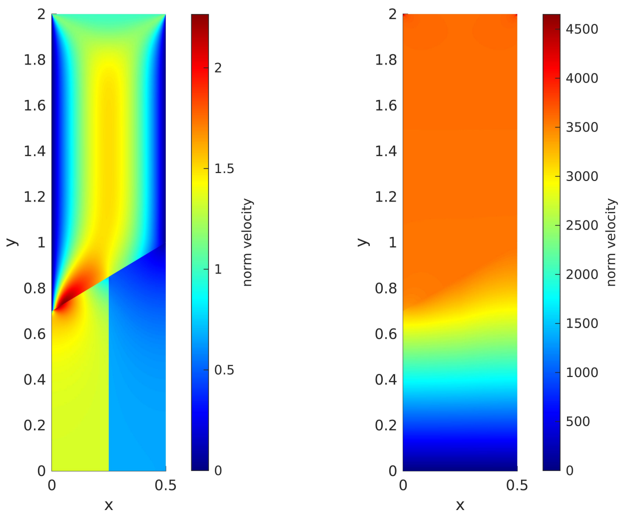

(a) Norm velocity (b) Pressure

Figure 4: Norm of velocity and flow vectors for numerical solution on discontinuous porous medium

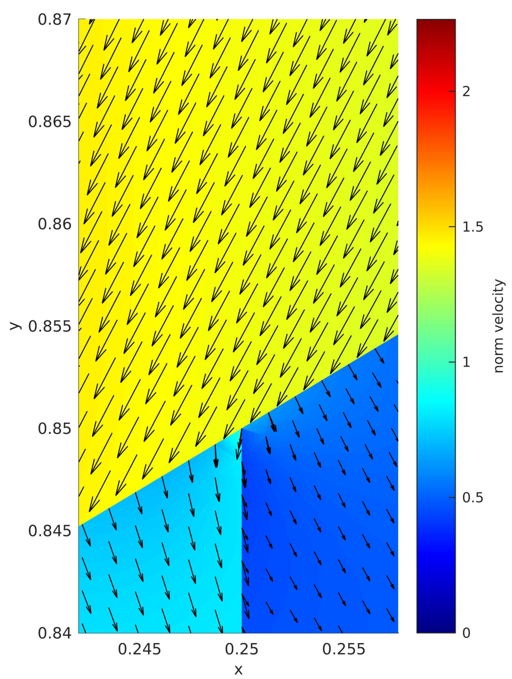

Figure 5: Zoom of vector fields near interface

References

[1] Abouorm, L., Troian, R., Drapier, S., Bruchon, J., Moulin, N., 2014. Stokes–Darcy coupling in severe regimes using multiscale stabilisation for mixed finite elements: Monolithic approach versus decoupled approach. European Journal of Computational Mechanics 23 (3-4), 113–137.

[2] Amestoy, P. R., Duff, I. S., L'Excellent, J.-Y., Koster, J., 2001. A fully asynchronous multifrontal solver using distributed dynamic scheduling. SIAM Journal on Matrix Analysis and Applications 23 (1), 15–41.

[3] Amestoy, P. R., Guermouche, A., L'Excellent, J.-Y., Pralet, S., 2006. Hybrid scheduling for the parallel solution of linear systems. Parallel Computing 32 (2), 136–156.

[4] Arnold, D. N., 1982. An interior penalty finite element method with discontinuous elements. SIAM Journal on Numerical Analysis 19 (4), 742–760.

[5] Arnold, D. N., Brezzi, F., Fortin, M., 1984. A stable finite element for the Stokes equations. Calcolo 21 (4), 337–344.

[6] Baumann, C. E., Oden, J. T., 1999. A discontinuous hp finite element method for convection-diffusion problems. Computer Methods in Applied Mechanics and Engineering 175 (3), 311–341.

[7] Beavers, G. S., Joseph, D. D., 1967. Boundary conditions at a naturally permeable wall. Journal of Fluid Mechanics 30 (01), 197–207.

[8] Bukač, M., Yotov, I., Zakerzadeh, R., Zunino, P., 2015. Partitioning strategies for the interaction of a fluid with a poroelastic material based on a Nitscheś coupling approach. Computer Methods in Applied Mechanics and Engineering 292, 138–170.

[9] Cai, M., Mu, M., 2012. A multilevel decoupled method for a mixed Stokes/Darcy model. Journal of Computational and Applied Mathematics 236 (9), 2452–2465.

[10] Cai, M., Mu, M., Xu, J., 2009. Numerical solution to a mixed Navier–Stokes/Darcy model by the two-grid approach. SIAM Journal on Numerical Analysis 47 (5), 3325–3338.

[11] Cao, Y., Chu, Y., He, X., Wei, M., 2013. Decoupling the stationary Navier–Stokes-Darcy system with the Beavers-Joseph-Saffman interface condition. In: Abstract and Applied Analysis. Vol. 2013. Hindawi Publishing Corporation.

[12] Cao, Y., Gunzburger, M., He, X., Wang, X., 2011. Robin-Robin domain decomposition methods for the steady-state Stokes–Darcy system with the Beavers–Joseph interface condition. Numerische Mathematik 117 (4), 601–629.

[13] Cao, Y., Gunzburger, M., He, X., Wang, X., 2014. Parallel, non-iterative, multi-physics domain decomposition methods for time-dependent Stokes–Darcy systems. Mathematics of Computation 83 (288), 1617–1644.

[14] Çeşmelioğlu, A., Girault, V., Rivière, B., 2013. Time-dependent coupling of Navier-Stokes and Darcy flows. ESAIM: Mathematical Modelling and Numerical Analysis 47 (02), 539–554.

[15] Çeşmelioğlu, A., Rivière, B., 2009. Primal discontinuous Galerkin methods for time-dependent coupled surface and subsurface flow. Journal of Scientific Computing 40 (1-3), 115–140.

[16] Chen, J., Sun, S., Wang, X.-P., 2014. A numerical method for a model of two–phase flow in a coupled free flow and porous media system. Journal of Computational Physics 268, 1–16.

[17] Chidyagwai, P., 2010. Coupling Surface Flow with Porous Media Flow. Ph.D. thesis, Rice University.

[18] Chidyagwai, P., Rivière, B., 2009. On the solution of the coupled Navier–Stokes and Darcy equations. Computer Methods in Applied Mechanics and Engineering 198 (47), 3806–3820.

[19] Chidyagwai, P., Rivière, B., 2010. Numerical modelling of coupled surface and subsurface flow systems. Advances in Water Resources 33 (1), 92–105.

[20] Chidyagwai, P., Rivière, B., 2011. A two-grid method for coupled free flow with porous media flow. Advances in Water Resources 34 (9), 1113–1123.

[21] Ciarlet, P. G., 1978. The Finite Element Method for Elliptic Problems. Elsevier.

[22] Dai, X., Cheng, X., 2008. A two–grid method based on Newton iteration for the Navier–Stokes equations. Journal of Computational and Applied Mathematics 220 (1–2), 566–573.

[23] Dawson, C., Sun, S., Wheeler, M. F., 2004. Compatible algorithms for coupled flow and transport. Computer Methods in Applied Mechanics and Engineering 193 (23), 2565–2580.

[24] Diegel, A. E., Feng, X. H., Wise, S. M., 2015. Analysis of a mixed finite element method for a Cahn–Hilliard–Darcy–Stokes system. SIAM Journal on Numerical Analysis 53 (1), 127–152.

[25] Discacciati, M., 2004. Domain Decomposition Methods for the Coupling of Surface and Groundwater Flows. Ph.D. thesis, École Polytechnique Fédérale De Lausanne.

[26] Discacciati, M., 2005. Iterative methods for Stokes/Darcy coupling. In: Domain Decomposition Methods in Science and Engineering. Springer, pp. 563–570.

[27] Discacciati, M., Gervasio, P., Giacomini, A., Quarteroni, A., 2016. The interface control domain decomposition method for Stokes–Darcy coupling. SIAM Journal on Numerical Analysis 54 (2), 1039–1068.

[28] Discacciati, M., Quarteroni, A., 2009. Navier–Stokes/Darcy coupling: modeling, analysis, and numerical approximation. Revista Matemática Complutense 22 (2), 315–426.

[29] Du, G., Hou, Y., Zuo, L., 2015. Local and parallel finite element methods for the mixed Navier–Stokes/Darcy model. International Journal of Computer Mathematics, 1–18.

[30] Girault, V., Rivière, B., 2009. DG approximation of coupled Navier–Stokes and Darcy equations by Beaver-Joseph-Saffman interface condition. SIAM Journal on Numerical Analysis 47 (3), 2052–2089.

[31] Hadji, M., Assala, A., Nouri, F., 2015. A posteriori error analysis for Navier–Stokes equations coupled with Darcy problem. Calcolo 52 (4), 559–576.

[32] Han, D., Sun, D., Wang, X., 2014. Two–phase flows in karstic geometry. Mathematical Methods in the Applied Sciences 37 (18), 3048–3063.

[33] Han, D., Wang, X., Wu, H., 2014. Existence and uniqueness of global weak solutions to a Cahn–Hilliard–Stokes–Darcy system for two phase incompressible flows in karstic geometry. Journal of Differential Equations 257 (10), 3887–3933.
[34] He, X., Li, J., Lin, Y., Ming, J., 2015. A domain decomposition method for the steady-state Navier–Stokes–Darcy model with Beavers–Joseph interface condition. SIAM Journal on Scientific Computing 37 (5), S264–S290.
[35] He, Y., Li, J., 2007. A multi-level discontinuous Galerkin method for solving the stationary Navier-Stokes equations. Nonlinear Analysis: Theory, Methods & Applications 67 (5), 1403–1411.
[36] He, Y., Liu, K.-M., 2005. A multilevel finite element method in space-time for the Navier-Stokes problem. Numerical Methods for Partial Differential Equations 21 (6), 1052–1078.
[37] Hou, J., Qiu, M., He, X., Guo, C., Wei, M., Bai, B., 2016. A Dual–Porosity–Stokes model and finite element method for coupling Dual-Porosity flow and free flow. SIAM Journal on Scientific Computing 38 (5), B710–B739.
[38] Hou, Y., 2016. Optimal error estimates of a decoupled scheme based on two-grid finite element for mixed Stokes–Darcy model. Applied Mathematics Letters 57, 90–96.
[39] Huang, P., Cai, M., Wang, F., 2016. A Newton type linearization based two grid method for coupling fluid flow with porous media flow. Applied Numerical Mathematics 106 (C), 182–198.
[40] Jäger, W., Mikelić, A., 1996. On the boundary conditions at the contact interface between a porous medium and a free fluid. Annali della Scuola Normale Superiore di Pisa-Classe di Scienze 23 (3), 403–465.
[41] Jia, H., Jia, H., Huang, Y., 2016. A modified two-grid decoupling method for the mixed Navier–stokes/Darcy model. Computers & Mathematics with Applications 72 (4), 1142–1152.
[42] Layton, W., 1993. A two-level discretization method for the Navier–Stokes equations. Computers & Mathematics with Applications 26 (2), 33–38.
[43] Layton, W., Lee, H., Peterson, J., 1998. Numerical solution of the stationary Navier-Stokes equations using a multilevel finite element method. SIAM Journal on Scientific Computing 20 (1), 1–12.
[44] Layton, W., Lenferink, H., 1996. A multilevel mesh independence principle for the Navier–Stokes equations. SIAM Journal on Numerical Analysis 33 (1), 17–30.
[45] Lee, H., 2004. A multigrid method for viscoelastic fluid flow. SIAM Journal on Numerical Analysis 42 (1), 109–129.
[46] Mu, M., Xu, J., 2007. A two-grid method of a mixed Stokes–Darcy model for coupling fluid flow with porous media flow. SIAM Journal on Numerical Analysis 45 (5), 1801–1813.
[47] Nassehi, V., 1998. Modelling of combined Navier–Stokes and Darcy flows in crossflow membrane filtration. Chemical Engineering Science 53 (6), 1253–1265.
[48] Rivière, B., 2008. Discontinuous Galerkin Methods For Solving Elliptic And Parabolic Equations: Theory and Implementation. Society for Industrial and Applied Mathematics.
[49] Rivière, B., 2014. Discontinuous finite element methods for coupled surface-subsurface flow and transport problems. In: Recent Developments in Discontinuous Galerkin Finite Element Methods for Partial Differential Equations. Springer, pp. 259–279.
[50] Rivière, B., Wheeler, M. F., Girault, V., 1999. Improved energy estimates for interior penalty, constrained and discontinuous Galerkin methods for elliptic problems. Part I. Computational Geosciences 3 (3-4), 337–360.
[51] Saffman, P., February 1971. On the boundary condition at the surface of a porous medium. Journal of Fluid Mechanics 2, 93–101.
[52] Shan, L., Zheng, H., Layton, W. J., 2013. A decoupling method with different subdomain time steps for the nonstationary Stokes–Darcy model. Numerical Methods for Partial Differential Equations 29 (2), 549–583.
[53] Shen, Y.-j., Han, D.-f., Shao, X.-p., 2015. Modified two-grid method for solving coupled Navier–Stokes/Darcy model based on Newton iteration. Applied Mathematics-A Journal of Chinese Universities 30 (2), 127–140.
[54] Temam, R., 1984. Navier–Stokes equations: Theory and Numerical Analysis. Vol. 343. AMS Chelsea Publishing.
[55] Wheeler, M. F., 1978. An elliptic collocation-finite element method with interior penalties. SIAM Journal on Numerical Analysis 15 (1), 152–161.
[56] Younes, A., Ouali, Y., 2014. The coupling Navier-Stokes/Darcy systems by vorticity-velocity-pressure formulation. Global Journal of Mathematical Analysis 2 (3), 80–90.
[57] Zhang, T., Yuan, J., 2014. Two novel decoupling algorithms for the steady Stokes–Darcy model based on two-grid discretizations. Discrete & Continuous Dynamical Systems-Series B 19 (3), 849–865.
[58] Zhao, X., Li, J., Su, J., Lei, G., 2013. Analysis of Newton multilevel stabilized finite volume method for the three-dimensional stationary Navier-Stokes equations. Numerical Methods for Partial Differential Equations 29 (6), 2146–2160.
[59] Zuo, L., Hou, Y., 2014. A decoupling two-grid algorithm for the mixed Stokes–Darcy model with the Beavers–Joseph interface condition. Numerical Methods for Partial Differential Equations 30 (3), 1066–1082.
[60] Zuo, L., Hou, Y., 2015. Numerical analysis for the mixed Navier–Stokes and Darcy problem with the Beavers–Joseph interface condition. Numerical Methods for Partial Differential Equations 31 (4), 1009–1030.
[61] Zuo, L., Hou, Y., 2015. A two-grid decoupling method for the mixed Stokes–Darcy model. Journal of Computational and Applied Mathematics 275, 139–147.